IMSE

Institute for Materials Science and Engineering

FRACTURE AND DEFORMATION

NAS-NRC
Assessment Panel
January 20-21, 1987

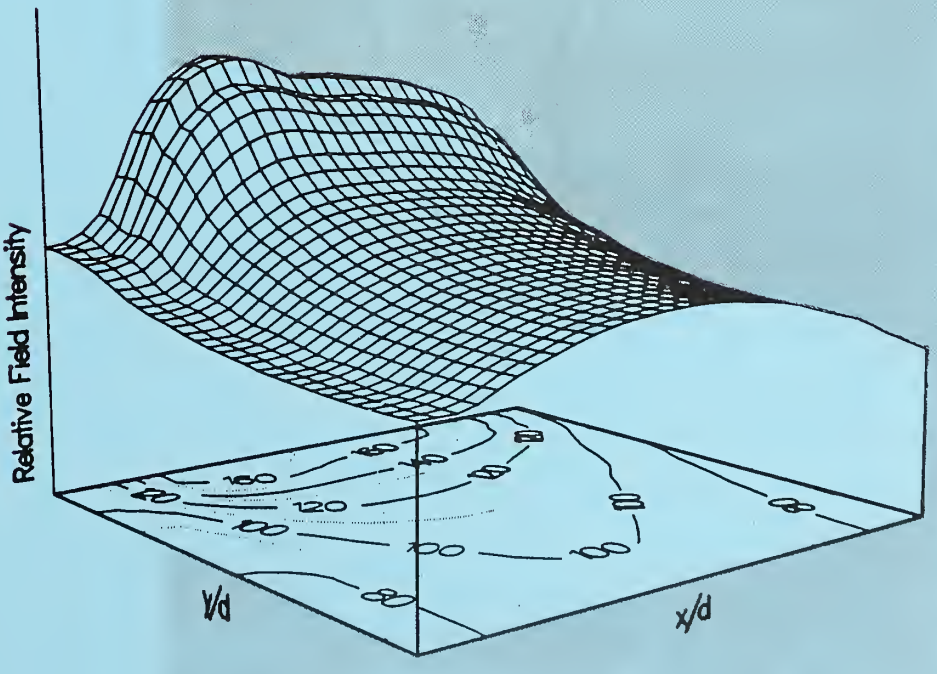

NBSIR 86-3436
U.S. Department of Commerce
National Bureau of Standards

Technical Activities 1986

Two-dimensional maps of the tangential component of the magnetic field intensity for two eddy current probes fabricated at NBS. For quantitative eddy current NDE, it is advantageous to have a spatially uniform magnetic field. The figures show the field distributions between the two feet of horseshoe-shaped ferrite probes. For one probe, the pole tips have a rectangular cross-section; for the other, the pole tips have a curved shape to improve the uniformity of the field. These probes have been used in a program to develop inversion methods for determining the size of small surface-connected flaws in advanced aerospace alloys.

Institute for Materials Science and Engineering

FRACTURE AND DEFORMATION

R.P. Reed, Chief
H.I. McHenry, Deputy

NAS-NRC
Assessment Panel
January 20-21, 1987

NBSIR 86-3436
U.S. Department of Commerce
National Bureau of Standards

DIVISION ORGANIZATION

Richard P. Reed Chief (303) 497-3870	Harry I. McHenry Deputy (303) 497-3268

ELASTIC-PLASTIC FRACTURE MECHANICS

Fracture Mechanics	David T. Read (303) 497-3853
Nondestructive Evaluation	Alfred V. Clark, Jr. (303) 497-3159
Welding	Thomas A. Siewert (303) 497-3523

FRACTURE MECHANISMS AND ANALYSIS

Fracture Physics	Ing-Hour Lin (303) 497-5791
Time-Dependent Properties	Richard J. Fields (301) 921-2980
Composite Mechanics	Maurice B. Kasen (303) 497-3558
Mechanical Metallurgy	George E. Hicho (301) 921-2989
Physical Properties	Hassel M. Ledbetter (303) 497-3443
Material Performance	Bruce W. Christ (303) 497-3424

ADMINISTRATIVE SUPPORT

Administrative Officer	Kathy Sherlock (303) 497-3288
Division Secretary	JoAnne Bean (303) 497-3251
Group Secretaries, Boulder	Becky Stevenson (303) 497-5338
	Chris King (303) 497-3290
Group Secretary, Gaithersburg	Judith Vaughan (301) 921-2951

CONTENTS

INTRODUCTION

Our principal goal is to establish the scientific basis to minimize material failure. Emphasis is placed on elastic and plastic deformation and fracture mechanics; materials include primarily structural alloys, composites, and weldments. Improvement in mechanical performance of materials is achieved by:

1. Theory and modeling of deformation and fracture, which lead to a fundamental understanding of the mechanisms of material mechanical response.

2. Characterization of mechanical performance, which is essential for the proper development and selection of materials for service applications and for efficient design that takes full advantage of material performance.

3. Development and application of fracture mechanics, which provide quantitative assessment and standards for the integrity of critical structures by considering material properties, flaw characterization, and service environment.

A recent study by our division concluded that in the United States costs of over $119 billion per year (1982 dollars) are associated with fracture. Design, structural codes and standards, material processing, quality control and inspection, and the replacement, inconvenience, injuries, and deaths from unexpected failures contribute to this cost. A significant cost associated with fracture is borne by the automotive industry (estimated at over $11 billion per year). One of our staff, B. W. Christ, spent this past year at Ford Motor Company in Detroit, where he worked with their staff to identify reducible costs and suggested means to minimize these costs.

The technical outputs of the division assist many government agencies, especially the Departments of Energy, Transportation, Defense, and Interior and the Nuclear Regulatory Commission. Our contributions to fusion energy research include low-temperature studies on austenitic stainless steels and composites for structural containment of the large magnetic fields produced by superconducting magnets. The development of unique spectrum-loading fatigue capabilities enables us to study steels for offshore structures in a simulated ocean environment. Mechanical-property and microstructural characterization and nondestructive inspection of steels for pressure-tank cars and railroad wheels, fracture-mechanics assessment of tank-car behavior, and numerous structural-metal fracture analyses assist the railroad industry. Research for the Department of Defense is diverse: We are helping the Navy to upgrade fracture-control plans; developing a new laboratory-size, crack-arrest test for characterization of ship plate; and conducting large-scale, J-integral panel tests on high-strength, low-alloy steels. Our dynamic crack arrest experiments on 10-m-long test panels have given us recognition as a large-scale fracture mechanics test laboratory and as a vital component in the national program of the Nuclear Regulatory Commission to set crack-arrest standards for the nuclear industry.

Dissemination of the results of recent materials research is an important function of our division. With the U.S. Department of Energy, we host the annual Cryogenic Structural Materials Workshop. We actively lead and support the biennial International Cryogenic Materials Conference. During the past

year we sponsored an international workshop on Quality in Underwater Welding of Marine Structures, in cooperation with the U.S. Department of the Interior and Colorado School of Mines, and a workshop on Computerization of Welding Data, in cooperation with the American Welding Institute. Our staff in Colorado organized the ASTM Eighteenth National Symposium on Fracture Mechanics; they are also editing the proceedings. We continue to expand and update the Materials Handbook for Fusion Energy Systems, and together with national welding organizations, we are creating a national welding data base.

We have unique mechanical property test facilities with an extensive range of capabilities: temperature -- 4 to 1500 K; specimen size -- 200 μm to over 15 m in length; load capacity -- 0.2 to 3,000,000 kg. In Boulder, we are now constructing a new laboratory wing to house a 450,000-kg-capacity, servo-hydraulic fatigue machine.

Research in our division is divided into two principal areas, which are discussed in depth in the Technical Activities section:

1. Elastic-Plastic Fracture Mechanics, which is the basis for the application of quantitative fitness-for-service criteria to the codes and standards of critical structures, and research in welding and nondestructive evaluation.

2. Fracture Mechanisms and Analysis, which encompasses research on fracture physics and mechanical and physical properties in support of advancing technologies and analyses of the failure causes of major national structural catastrophies.

R. P. Reed
Chief
Fracture and Deformation Division

RESEARCH STAFF

Arvidson, John M.	• Mechanical properties at cryogenic temperatures • Test systems for cryogenics
Austin, Mark W.	• Elastic properties • X-ray diffraction applied to stacking-fault energy, internal strain, texture
Cheng, Yi-Wen	• Fatigue of metals • Fracture behavior of surface flaws • Fatigue-life predictions • Thermomechanical processing of steels
Christ, Bruce W.	• Data-base management • Failure analysis of engineering structures • Mechanical properties of structural metals • Mechanical durability of motor vehicles
Clark, Alfred V., Jr.	• Theoretical and experimental ultrasonics • Engineering mechanics • Nondestructive evaluation
Crooks, Mary J.	• Ferrous metallurgy • Failure analysis • Microstructural characterization
deWit, Roland	• Defect theory • Fracture mechanics
Fields, Richard J.	• Mechanical properties • High-temperature materials
Hicho, George E.	• Mechanical metallurgy • Ferrous metallurgy • Failure analysis • Preparation and certification of standard reference materials
Kasen, Maurice B.	• Composites at low temperatures • Grain boundary segregation • Welding metallurgy of aluminum
Kriz, Ronald D.	• Development of finite-element analysis for composites • Mechanics of composite materials • NDE of composite materials

Ledbetter, Hassel M.	• Physical properties of solids • Theory and measurement of elastic constants • Physical properties of austenitic steels • Measurement and modeling of physical properties of composite materials • Martensite-transformation theory
Lin, Ing-Hour	• Fracture-toughening mechanisms • Ductile-brittle transition • Elastic interactions of cracks and defects • Dynamic deformation and fracture • Theory of dislocations and strengthening mechanisms
Low, Samuel R., III	• Mechanical testing • Instrumentation for dynamic measurements
McHenry, Harry I.	• Fracture mechanics • Low-temperature materials • Fracture control
Moulder, John C.	• Eddy-current measurement and theory • Ultrasonic measurement of residual stress • Optical methods for full-field strain analysis
Purtscher, Pat T.	• Fracture properties of high-strength steels • Metallography and fractography using light and electron microscopy • Mechanical and fracture toughness test methods
Read, David T.	• Physics of deformation and fracture • Elastic-plastic fracture mechanics, analysis and test methods • Mechanical properties of metals
Reed, Richard P.	• Mechanical properties • Low-temperature materials • Martensitic transformations
Schramm, Raymond E.	• Ultrasonic NDE of welds • Ultrasonic measurement of residual stress • Design of EMATs
Scull, Lonnie L.	• Mechanical properties of metals, foams, composites, and ceramics at low temperatures • Metal processing

Shives, Robert T.	• Hardness test methods • Mechanical properties • Failure analysis
Siewert, Thomas A.	• Welding metallurgy of steel • Gas-metal interactions during welding • Welding data-base management
Simon, Nancy J.	• Information retrieval and data-base management of properties of materials at low temperatures • Compilation of structural alloy properties at low temperatures for handbook
Tobler, Ralph L.	• Fracture mechanics • Fatigue crack growth resistance at low temperatures • Low-temperature test standards
Walsh, Robert P.	• Mechanical properties at low temperatures • Design and development of mechanical test equipment

TECHNICAL ACTIVITIES

ELASTIC-PLASTIC FRACTURE MECHANICS

This task addresses establishment of a scientific basis for the development of fracture prevention requirements for structural materials that exhibit plastic fracture behavior. Safety and durability are primary considerations in the design and construction of engineering structures. Sophisticated methods to assess structural safety and durability have been developed on the basis of linear elastic fracture mechanics. These analytical methods are applicable to the high-strength alloys used for aerospace vehicles and to the heavy-section steels used for nuclear pressure vessels. Unfortunately, the methods of linear elastic fracture mechanics do not apply to a wide range of metal structures, including bridges, pressure vessels, ships, offshore structures, and pipelines, because in these applications, the materials of construction (typically steels and aluminum alloys) are highly plastic (nonlinear) before fracture. Consequently, the assessments of their structural safety and durability are based on empirical methods and prior experience. Although current methods usually provide a reasonable record of structural safety, improved efficiency and productivity could be achieved if more rational methods were used to establish material-toughness requirements, allowable stress levels, minimum service temperatures, and weld-quality standards.

Modeling of critical structures to assess their fitness for service requires knowledge of the mechanical properties, flaw sizes, and operating stresses of the structural materials and welds. Fundamental knowledge is also required to relate these parameters to crack initiation and growth. This task combines the studies of elastic-plastic fracture toughness, fatigue, nondestructive inspection, stress analysis, and welding to develop elastic-plastic fracture mechanics.

Representative Accomplishments

- Data from full-field video-optical strain measurements on a single-edge-cracked tensile panel of a high-strength, low-alloy steel were used to calculate Rice's J-integral for a variety of integration paths enclosing the crack tip. The mathematical proof of the path independence of the J-integral assumes nonlinear elastic material behavior, but real metals have incremental plastic behavior. Experimental path independence in real metals is essential if this measurement technique is to be useful for obtaining accurate values of the J-integral. No path dependence was found from these measurements.

- Four wide-plate crack-arrest tests were completed; two were performed on as-received A533B steel and two on a steel that had been heat-treated to simulate radiation embrittlement. Results showed that cleavage fracture could occur at temperatures above the onset of upper-shelf behavior as determined by traditional impact testing. To the dynamic-strain data

obtained from these tests, we applied a new fracture-mechanics analysis procedure that we developed to calculate the stress-intensity factor, K_D, and crack velocity, å. The K_D increased moderately while å was near its maximum value of 600 m/s, but as å decreased, K_D increased rapidly to an extraordinarily high value at crack arrest.

- A velocity-and-time-interval measurement system that has a precision of ± 1 ns or better has been developed. The system currently uses electromagnetic acoustic transducers (EMATs) to transmit and receive shear waves in metals. It has a variety of applications; for example, in measuring residual stresses by the acoustic birefringence method. Residual stresses due to welding thin aluminum plates measured with this method were found to be within 20 MPa of strain-gage values. Residual stresses due to multipass welds in thick (51-mm) steel plates are currently being measured. The state of residual stresses in the rim of drag-braked railroad wheels has also been characterized. The system is also being used to measure texture in rolled aluminum alloy plates. In this application, it serves as a prototype for on-line process control for texture monitoring of material used for can manufacture.

- EMATs were used to size inadequate-fusion flaws in welds. The interaction of ultrasound with these flaws is complex, since the flaws are at an angle to the incident ultrasonic field. We developed a preliminary flaw-sizing algorithm, which gave encouraging results when applied to measurement of well-characterized inadequate-fusion flaws in weldments provided by our welding group. Because crack closure can have an effect on ultrasonic flaw sizing, we compared the effects of closure on flaw sizing using conventional high-frequency piezoelectric transducers and EMATs. Test results revealed an upper limit to flaw-sizing error when using low-frequency (500 kHz) EMATs.

Fracture Mechanics

D. T. Read, J. F. Cardenas-Garcia,[1] Y.-W. Cheng, J. D. McColskey,
H. I. McHenry, J. C. Moulder, B. Petrovski,[2] P. T. Purtscher, R. L. Tobler

[1]Guest Worker, Colorado State University, Fort Collins, Colorado
[2]Guest Worker, University of Belgrade, Belgrade, Yugoslavia

Our studies focus on (1) the growth of cracks by fatigue, (2) the relationship between crack size, applied stress or strain, and the static and dynamic driving force for fracture, (3) static and dynamic fracture toughness, and (4) applications of fracture mechanics to assess the safety of actual structures and to investigate causes of failure.

Fracture mechanics relates the fracture resistance of a material containing a crack to the stress and strain fields in the vicinity of the crack. Fracture occurs when the crack-tip strain fields reach a magnitude that exceeds the material's resistance to fracture. Determination of the critical conditions is complicated by the numerous variables that influence the fracture process. Because modern structural metals are sufficiently tough that fracture rarely occurs under linear elastic strain conditions, we have concentrated on fracture under conditions of plastic strain at and near the crack tip.

Fracture toughness

Fracture is prevented as long as the material fracture toughness exceeds the driving force for fracture. Crack-driving force under static elastic-plastic conditions is measured by the J-integral or the crack-tip opening displacement (CTOD). These parameters characterize the stress and strain fields around a crack tip in different ways. Under highly dynamic conditions, plastic strains are suppressed; so the crack-tip fields are linear elastic and can be characterized by the dynamic Mode I stress-intensity factor, K_D.

Driving force for fracture in mismatched weldments. Static-fracture driving forces were measured, by using the experimental technique of direct measurement of the J-integral, in a series of welded tensile panel specimens with varying amounts of mismatch between the strengths of the weld and base metal. This year's effort was a continuation of a previous study in which small and large cracks were placed in the center of three types of welds, which were designated undermatched, normal matched, and overmatched. This year the small and large cracks were placed in the heat-affected zone (HAZ) of the same three weld types. The HAZ results generally confirmed the weld center results, with some differences in the specifics of the behavior.

As before, the overmatched weld shielded the small crack from the plastic strains. The normal-matched weld with a small crack in its HAZ was also shielded from the strains, although another specimen of the same type with a crack in the weld center was not. The shielding effect was observed for the large crack in the HAZ of the overmatched weld, another difference from the behavior of cracks in the weld center, where no shielding was observed for large cracks. This enhanced shielding behavior for cracks in the HAZ may

indicate that HAZ material is slightly stronger than the weld center, but it is impossible to measure the strength properties of the HAZ with any known tensile test technique. This suggests that HAZ behavior is a candidate for investigation by finite-element modeling of the weldment as a whole. Another observed difference between HAZ and weld center cracks was that marginally unstable tearing behavior was observed for the large crack in the undermatched HAZ. This behavior was attributed to the lower toughness of the HAZ as compared to that of the weld center. It is interesting because one of the goals of elastic-plastic fracture mechanics is predicting the onset of unstable behavior. No predictions were made in this case, but the observed results could be applicable to verification of models of instability.

J-integral from full-field strains. The full-field video-optical strain measurement technique developed in our division enabled us to obtain crack-driving force as measured by the J-integral for a double-edge-notched specimen of high-strength, low-alloy (HSLA) steel. Several series of J-integral paths were compared, including paths with constant width, constant height, and constant aspect ratio. For one of the cracks, for which the data were better, the average J values of the various paths deviated from the grand average by an average of less than 6 percent. No systematic dependence of J on the size or shape of the integration path was found.

This result implies that the J-integral is experimentally path independent, a conclusion expected from the theoretical proof of path independence, even though the theoretical proof assumes nonlinear elastic material behavior, which is technically different from the actual incremental plastic material behavior. The full-field measurement of J agreed well with the value measured from strain-gage data and with an estimate based on the crack-mouth opening displacement. It also agreed with the value given by a semiempirical estimation scheme developed over the past five years in which J is proportional to the crack length, the remote strain, a collection of factors including the yield strength and Young's modulus, and a proportionality factor of 2.

Notch-tensile versus J-integral results at 4 K. The standard elastic-plastic fracture toughness test, which measures J_{Ic}, requires specialized equipment and is an expensive procedure, especially at liquid helium temperature. A simplified method of estimating fracture toughness is highly desirable. Inverse correlations between fracture toughness and yield strength have been reported previously, and such a correlation was found for a large data base of forty materials; however, this correlation was weak because of the effects of inclusion content and different levels of alloying.

The notch-tensile test has traditionally been used as a screening test of fracture toughness, especially in the aluminum industry. Therefore, we explored the possibility of estimating fracture toughness of austenitic stainless steels from the strength and ductility of the notch-tensile specimen. Sixteen of the forty materials were chosen on the basis of the completeness of their characterization. In spread-sheet format, we gathered all the relevant data -- yield strength, ultimate strength, notch-tensile strength,

displacement to fracture, and J-integral fracture toughness (measured on standard compact tensile specimens) -- and searched for a correlation between toughness and these properties.

For this data set, the expected correlation between fracture toughness and yield strength was poor because the sixteen materials had nearly the same yield strength. The product of notch-tensile strength and displacement to fracture correlated positively with the ratio of notch-tensile strength to yield strength, and both correlated with toughness, but with a large amount of scatter. Although we expected the product of notch-tensile strength and displacement to equal the J-integral toughness, the best-fit straight line for the plot of this product versus J-integral had a slope between 2 and 5. This result indicates (1) the high degree of scatter in the data and (2) the large effects of test variables, including crack sharpness and tensile versus bending loading mode. On the basis of these results, the standard test is still the only way to determine the J-integral toughness of an austenitic stainless steel at 4 K. Predicting the results of tests of other geometries from J_{Ic} data has not been thoroughly checked, but we expect considerable scatter in the correlations.

Toughness scatter in the ductile-brittle transition. Even standard toughness measurements of conventional ferritic steels in their ductile-to-brittle transition temperature range have considerable scatter. This scatter is usually rationalized as being caused by the distribution of weak metallurgical links that trigger the fracture. However, there are no reports of direct fractographic observation attributing fracture toughness variations to this cause. We are attempting to document this phenomena in a study of a pressure vessel steel quite similar to A533B, which is used in nuclear reactor containment vessels.

A preliminary study has shown that the toughness of this material is scattered in the temperature range -80°C to 0°C. Toughness variations of a factor of three have been observed at two temperatures within this interval. The high toughness values resulted after some ductile tearing. From scanning electron microscope observations, the fracture-initiating feature on the fracture surface was identified as an inclusion.

In the remainder of the program, we plan to test a statistically large sample of specimens at a selected temperature in the ductile-to-brittle transition temperature range. The fracture surfaces will be examined in the hope of correlating the various toughness values observed with the details of the fracture-triggering feature of the fracture surface.

Calculation of K_D from dynamic strain data. Calculation of crack-driving forces during a dynamic fracture event was made possible by the records of strain-gage data (see Fig. 1) from near the path of the dynamic crack in a wide-plate crack-arrest specimen (1 m by 10 m). Because the specimen plate was very large and because the crack ran at a nonrelativistic velocity (600 m/s, roughly 0.2 the speed of sound), the stress solution for a static crack in an infinite plate with a center crack was adopted. The dependence of strain on position was developed in terms of three adjustable parameters:

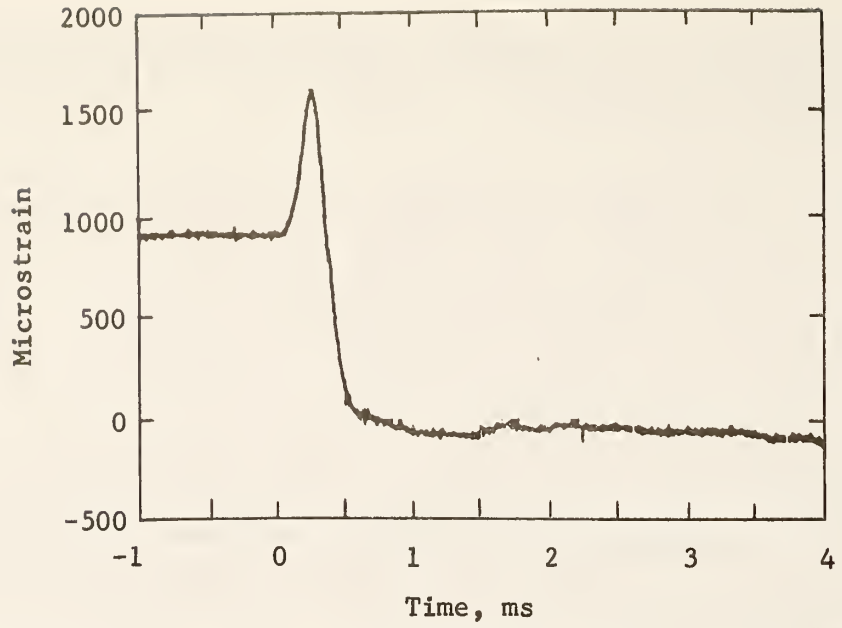

Fig. 1. Strain as a function of time after crack initiation measured by one of twenty strain gages located near the path of a crack running at 600 m/s. The peak occurs as the crack passes; the width of the peak is determined by the speed of the crack. Strain is lower after the crack passes because the crack creates a stress-free surface.

the crack-tip position; the stress-intensity factor, K; and the applied stress, σ. These three parameters were adjusted to best fit the measured instantaneous strain data at about twenty different times. As the crack runs, the location of the peak of the strain distribution moves along with the crack tip; the amplitude of this strain peak is proportional to K_D.

The fitted crack position values were plotted against time and differentiated to give crack-tip velocity. The crack was running in a temperature gradient; as the crack ran, the driving force increased because the crack length was increasing, and the material resistance increased because the temperature was increasing. At a crack length of about 0.5 m, the crack slowed and stopped. As it slowed, the driving force increased even more because the bulk of the plate had time to relax toward its static equilibrium position. Eventually, a large plastic zone was formed at the tip of the arrested crack, so that the linear elastic solution for the strains could no longer be used.

The calculated K_D values were compared with the crack-arrest toughness values obtained from compact crack-arrest tests of A533B specimens. The driving-force curve crossed (from over to under) the toughness curve at a crack length of approximately 0.5 m, which is where the crack arrested. This arrest at the location predicted by the toughness curve confirms the accuracy of both the toughness curve and the method of calculating K_D.

Double-tension crack-arrest test. The double-tension crack-arrest specimen previously developed by us has been used to compare two heats of HSLA plate. The running crack was arrested in a temperature gradient, which enabled us to measure the crack-arrest temperature. Ten thermocouples were mounted on each specimen. Crack initiation was achieved without projectiles or other inconvenient devices. A mechanical spring varied the load-train compliance, with no observed systematic effect on the crack-arrest temperature. Side grooves were cut in four of the six specimens to guide the running crack, but they will not be used in future tests because the crack is able to escape the side groove, which introduces an unwanted variable.

Three specimens of each heat were tested; the difference in crack-arrest temperatures for the two heats was significant. One heat produced arrest at an average temperature of -18°C, whereas the average arrest temperature in the three specimens from the other heat was 43°C. The difference in crack-arrest toughness between these two heats is attributed to metallurgical causes. The heat with the higher crack-arrest temperature was 2.6 cm thick; the other was only 2.0 cm thick. The thickness difference is significant because HSLA steel properties are sensitive to the degree of reduction in thickness achieved during processing. This test series demonstrated the convenience and utility of this test as a means of screening crack-arrest properties.

Compact crack-arrest test round robin. We participated in a round-robin test program in support of a proposed test standard for the compact crack-arrest test. The compact crack-arrest specimens, about 20 cm square by 5 cm thick, were wedge loaded. We recorded crack-mouth opening displacement and load for three specimens of A533B steel and three specimens of A588 steel. Most of the tests were invalid by the criteria of the proposed test method.

Fatigue crack growth

Crack initiation and growth under repeated loading is another key technological fracture problem; it also is not thoroughly understood on a first-principles basis. We are studying threshold behavior, small cracks, and random-load behavior.

Fatigue cracks are believed to grow only when the cyclic stress-intensity factor is higher than some threshold value characteristic of the material. Our automatic, computer-controlled fatigue testing system is one of two in the world with the capability of conducting threshold fatigue measurements at liquid helium temperature; it can measure fatigue crack-growth rates from 10^{-6} to 10^{-10} m (less than one lattice spacing) per load cycle in the temperature range 295 to 4 K.

Work on fatigue crack growth at plastically deformed regions has shown that the linear elastic fracture mechanics approach is applicable to analyzing the fatigue crack growth rates in these regions, provided that the local stress-strain relation remains linear under cyclic loading and the crack is long

enough to preclude small-crack behavior. Small cracks grow at higher rates than those predicted from da/dn-versus-ΔK results for long cracks. One can adjust for small-crack behavior by adding an intrinsic crack length to the physical crack length, as suggested by El Haddad.

Studies of random-load fatigue led to the development of procedures for predicting the growth rates of fatigue cracks under sea-wave loading. The procedures start with an anticipated stress spectrum acting on a component of interest. Fatigue crack growth rates are calculated by using the fracture mechanics approach and the equivalent-stress-range concept. Procedures for calculating the equivalent-stress ranges from a power spectrum density function or an exceedances spectrum, which describes the applied random loads, were also developed. The validity of the procedures has been verified by experiments that simulate power-spectra characteristics of the North Sea environment.

Several computer codes, which are commonly used in fatigue research, have been developed during the studies of random-load fatigue. These include codes for cycle counting in random loads, for simulating random loads from a power spectrum density function, and for controlling the automatic fatigue testing machine.

Thermomechanical processing of steels

Increasing the strength of a steel usually reduces its toughness. In ferritic steel, however, strength and toughness, especially low-temperature toughness, can be increased simultaneously if the strength is realized through ferritic grain refinement. To achieve the optimum combination of strength and toughness, it is essential to control and select the time-temperature-deformation schedule used for hot rolling. On the basis of fundamental metallurgical principles, the rolling schedule can be developed in the laboratory through a thermomechanical processing study.

A simulator has been designed and is being constructed in the division to study the thermomechanical processing of steels. It consists of a servohydraulic loading system, a vacuum system, an induction heater with gas cooling capability, a dilatometer for phase-transformation studies, and a computer system for process control and data handling, as shown in Fig. 2. The simulator will have the following features: 250-kN load capacity with a maximum actuator traveling speed of 50 cm/s; multiple-strike capability at different displacements and strain rates; a maximum heating rate of 150°C/s (with a cylindrical steel specimen of 1.2-cm diameter); and a maximum cooling rate of 30°C/s.

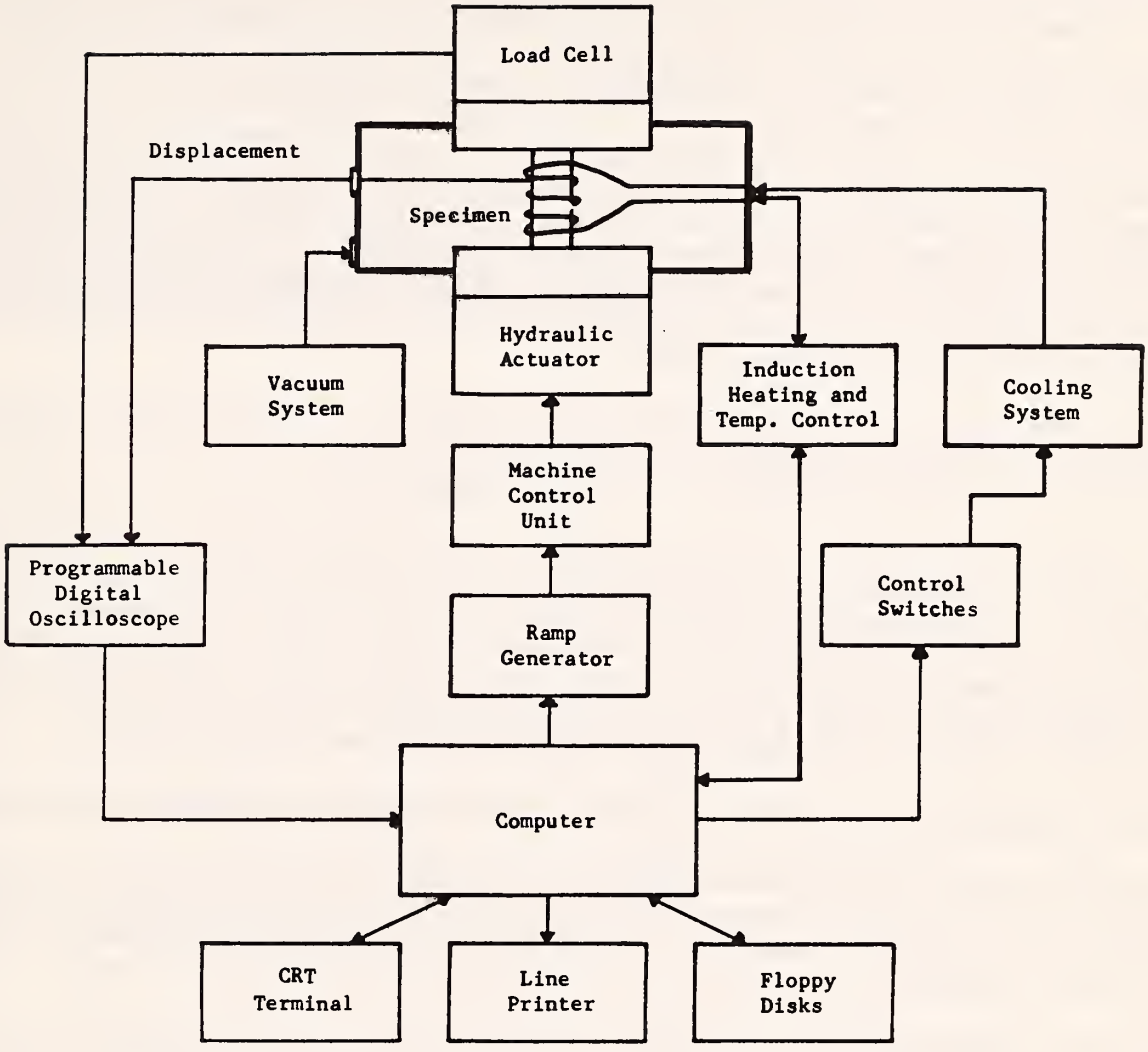

Fig. 2. Simulator designed at NBS for thermomechanical processing of steels.

Nondestructive Evaluation

A. V. Clark, Jr., D. Mitraković,[1] J. C. Moulder, R. E. Schramm, P. J. Shull

[1]Guest Worker, University of Belgrade, Belgrade, Yugoslavia

The NDE Group has been developing methods for using electromagnetic sensors in a variety of material characterization and nondestructive testing applications. Two primary sensor types are being used at present: electromagnetic-acoustic transducers (EMATs) and eddy-current probes. Both sensor types are noncontacting, and both can be easily and rapidly scanned over the material under investigation. These advantages indicate a potential for their use in industry as process-control sensors.

EMATs have been used to characterize the texture of aluminum plate, to characterize the state of stress in drag-braked railroad wheels, and to identify and size incomplete-fusion flaws in steel weldments.

Two types of eddy-current probe have been fabricated and their performance has been characterized. The uniform-field eddy-current probe generates a spatially uniform magnetic field; its use to interrogate flaws greatly simplifies the inversion model used to obtain flaw sizes. The reflection probe is a two-port device consisting of a drive coil encircling a differential pair of pickup coils; it has a very good signal-to-noise ratio and is relatively insensitive to variations in its height above the workpiece surface.

Electromagnetic-acoustic transducers: measurement of preferred orientation

The NDE Group is using electromagnetic-acoustic transducers (EMATs) to make quantitative ultrasonic measurements for the purpose of materials characterization. One such application is measurement of preferred orientation (texture) in rolled aluminum plates, which are used in the manufacture of cans.

Theories which model the influence of texture on ultrasound predict that the phase velocities in rolled steel and aluminum plates are influenced by the three lowest order orientation distribution coefficients (ODCs). These ODCs occur as multipliers in a series expansion for the orientation distribution function, which gives the probability that a crystallite (grain) will have a certain orientation relative to the plate axes. Consequently, the ODCs are quantitative measures of texture.

A proof-of-concept test was performed to examine the feasibility of ultrasonic texture monitoring in aluminum plates. Specimens of hot-rolled plate material to be used for can stock were obtained from actual production runs. Relative velocity measurements were made with surface (Rayleigh) waves, shear-horizontal waves (SH waves) and Lamb-wave modes (plate waves). In collaboration with researchers in industry, academia, and other government laboratories, experiments were made with different transducers and velocity measurement systems. The ODCs were then calculated from the measurements by using the relevant theoretical models.

Typical results for two ODCs, ω_{420} and ω_{440}, are shown in Fig. 3. It is evident that generally good agreement was obtained for measurements made at the different laboratories. This agreement is encouraging because (1) it indicates general agreement of the theories that model the influence of texture on sound velocity and (2) it indicates that results are not dependent upon the types of transducers and velocity measurement systems used.

Another trend evident in Fig. 3 is the sensitivity of ODCs to plate temperatures at the exit of the rolling mill. This is in qualitative agreement with metallurgical considerations. Neutron-diffraction pole figures have been made and a computer program is being developed (by the Mechanical Metallurgy Group) to obtain ODCs to compare with ultrasonic results.

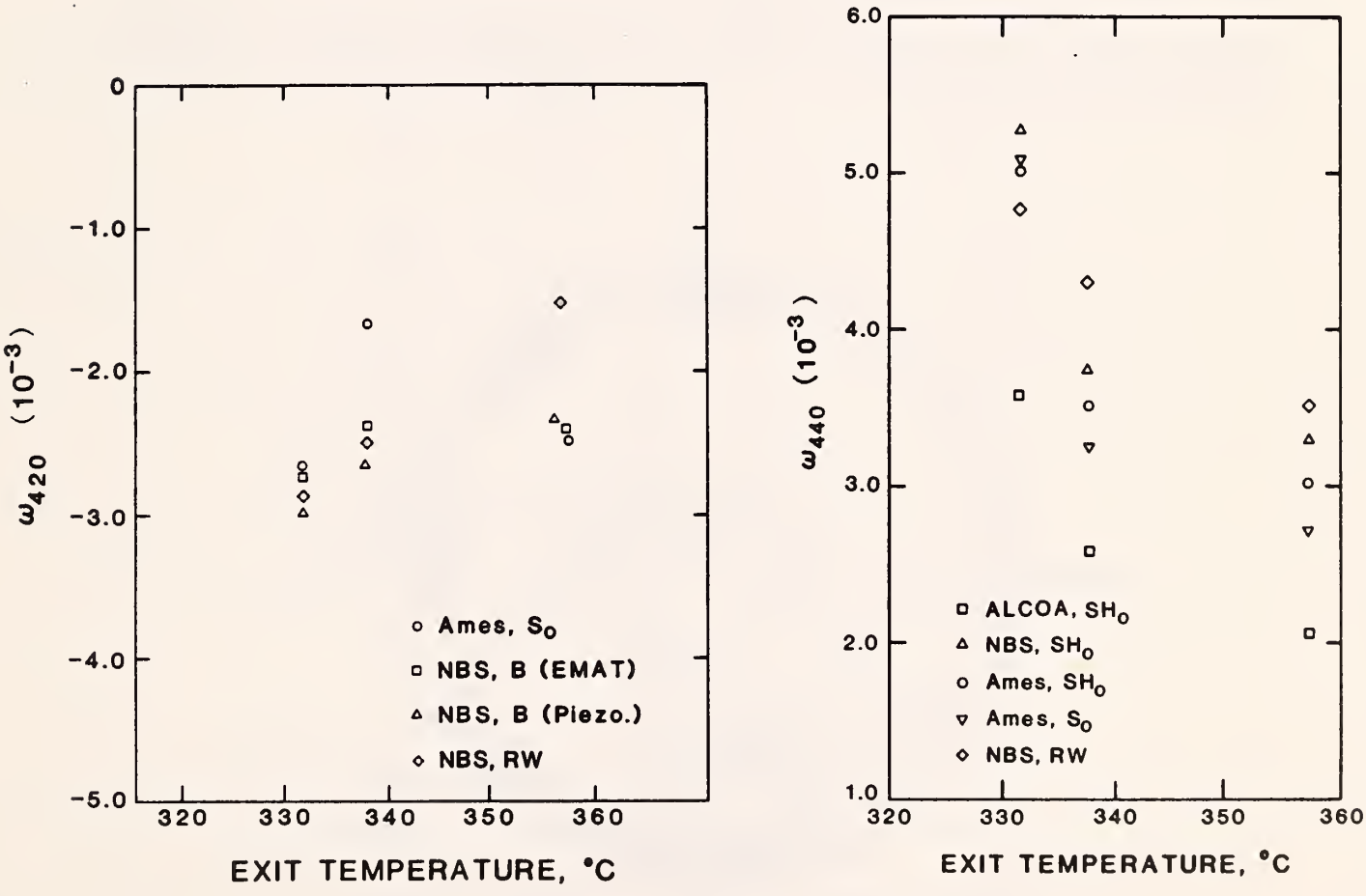

Fig. 3. Orientation distribution coefficients ω_{420} (a) and ω_{440} (b) for hot-rolled aluminum alloy plates with different exit temperatures. Measurements were made with the lowest order symmetrical Lamb-wave mode (S_0 mode), acoustic birefringence (B), Rayleigh waves (RW), and lowest order shear-horizontal wave plate mode (SH_0 mode). Acoustic birefringence was measured with both an EMAT and a conventional piezoelectric transducer. Measurements were performed at ALCOA, NBS, and Ames Laboratory (Iowa State).

Electromagnetic-acoustic transducers: **measurement of residual stress**

Proof-of-concept tests have also been performed to demonstrate the use of EMATs for residual stress measurements in drag-braked railroad wheels. Cast steel wheels were obtained from the Transportation Test Center (TTC) as part of an ongoing program there. One such wheel is shown in Fig. 4; it had been saw-cut as part of the TTC program. The hoop stress, the dominant stress, has been relieved at the saw cut.

Shear-horizontal waves were generated by EMATs and propagated through the rim of the wheel; the waves were polarized in the radial and hoop directions. The normalized difference in velocity of these waves is called the acoustic birefringence, B, and is related to the difference of principal stresses:

$$B = B_0 + C_a (\sigma_\theta - \sigma_r) .$$

Here B_0 is the unstressed birefringence due to texture (induced by casting the wheel), σ_θ and σ_r are hoop and radial stresses, respectively, and C_a is the stress-acoustic constant.

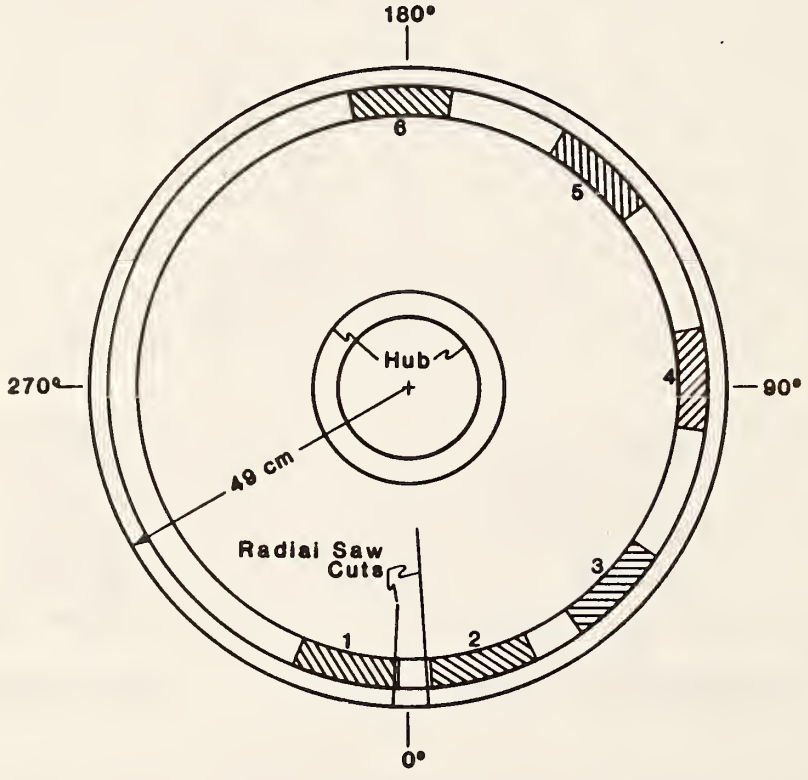

Fig. 4. Top view of a saw-cut railroad wheel. Angle θ is measured circumferentially around the rim. Shaded areas indicate where the rim was milled.

The values of B_0 were obtained by measuring the birefringence near the saw cuts. The birefringence was then measured at other locations around the rim and predictions were made of $\sigma_\theta - \sigma_r$. These values are shown in Fig. 5. For comparison, we have also included the results we obtained from a conventional piezoelectric transducer (made of PZT). This transducer had been used in similar experiments at Osaka University on rolled steel wheels of Japanese manufacture; results obtained with this device were within 40 MPa of stresses measured with destructive methods. Hence, we used the PZT transducer as a benchmark for EMAT results.

Good agreement between EMAT and PZT measurements is evident in Fig. 5 for regions where the rim had been milled (shaded regions in Fig. 4). Furthermore, EMAT measurements indicated relatively little sensitivity to surface preparation (little scatter about dashed line in Fig. 5). The latter result was quantified by varying the surface preparation on a second wheel. For

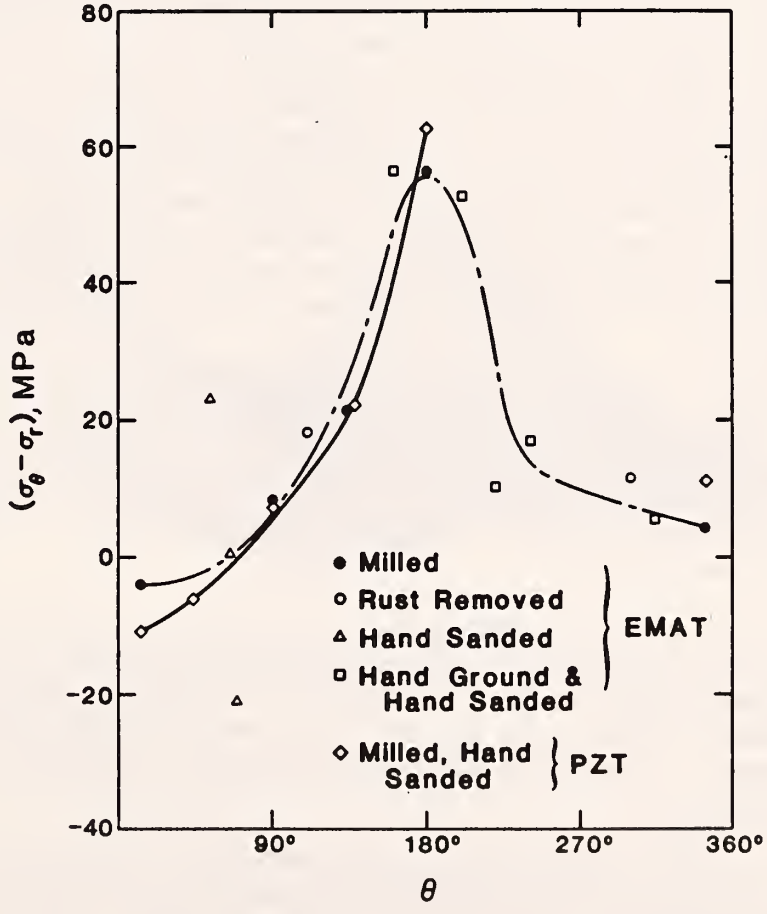

Fig. 5. Difference of principal stresses at various locations, θ, on the circumference of a saw-cut railroad wheel. EMAT measurements are shown for various surface preparation treatments.

treatments that varied from hand sanding to milling, the variability in EMAT measurements was equivalent to a stress uncertainty of only 25 MPa. This indicates that EMATs are more suitable for field use than piezoelectric transducers, which require careful surface preparation.

Electromagnetic-acoustic transducers: measurement of welding defects

Our work has continued on the use of EMATs for detecting and sizing planar defects in welded steel plates. We use transducers that generate SH waves at about 450 kHz. This ultrasound diffracts from the flaws; flaw depth is determined from measurements of signals that are back-scattered from and transmitted through the weld region. For flaws normal to the plate surface (e.g., inadequate penetration), our sizing capabilities extend from depths of about 0.5 to 12 mm in a 16-mm-thick plate.

Recent work has extended this technique to flaws canted with respect to the plate surface (e.g., incomplete fusion). The flaw-ultrasound interaction is more complicated in this case. Ultrasonic energy propagates along a plate in specific, allowed modes dependent on plate thickness and frequency. The constructive and destructive interference of these modes can lead to simple or complex signal shapes, depending on transducer locations. A combined theoretical and experimental program (in cooperation with faculty from the University of Colorado) guided us in selecting the EMAT placement for the greatest sensitivity and reliability in flaw detection and sizing. Despite the complexity, our measurements on actual flawed welds showed a good sizing capability for most of our test welds. There were some sections of the welds, however, where discrepancies were evident and not understood. More work will be necessary to determine the cause of these difficulties in particular regions.

The effect of closure due to applied or residual stresses is a potential problem in all NDE methods for the important case of planar flaws. In all methods, as the crack faces are pressed together, the probability of detection decreases. In ultrasonics, in particular, the effective acoustic-impedance mismatch between flaw region and base plate drops, as does the amplitude of the reflection.

To examine this effect, we made a special specimen that enabled us to apply a variable stress over a planar interface. We found that our EMAT-based flaw-sizing parameter (the ratio of back-scattered amplitude to transmitted amplitude) decreased by about 25 percent with applied load and then saturated at about this level. This gives us an indication of the magnitude of large stress-induced errors.

In the course of these crack-closure tests, we also measured the relative effects on our low-frequency EMAT-generated signal and a higher frequency signal from a piezoelectric transducer. In some cases, there was a notably larger drop in reflection for the higher frequency signal as the applied stress increased. This may be due to the size of the contact area between the two faces relative to the wavelength.

Eddy-current probes

In eddy-current testing, alternating currents are induced in the surface of a test piece with a small electromagnetic probe, usually consisting of a wire coil surrounding a ferrite core. Interaction of the induced surface currents with surface-connected flaws causes a change in the impedance of the coil, which can be detected with a measuring instrument connected to the input terminals of the probe. Since the magnitude of the impedance change is proportional to the square of the magnetic field strength, eddy-current probes are usually designed with the goal of achieving high field strengths in a small region. This results in highly nonuniform field distributions, which complicate the analysis of flaw signals.

A different approach, under development in the NDE Group, uses a probe with a spatially uniform magnetic field. This simplifies the analysis of field-flaw interactions and makes it much easier to analyze experimental results and determine flaw sizes from measurements.

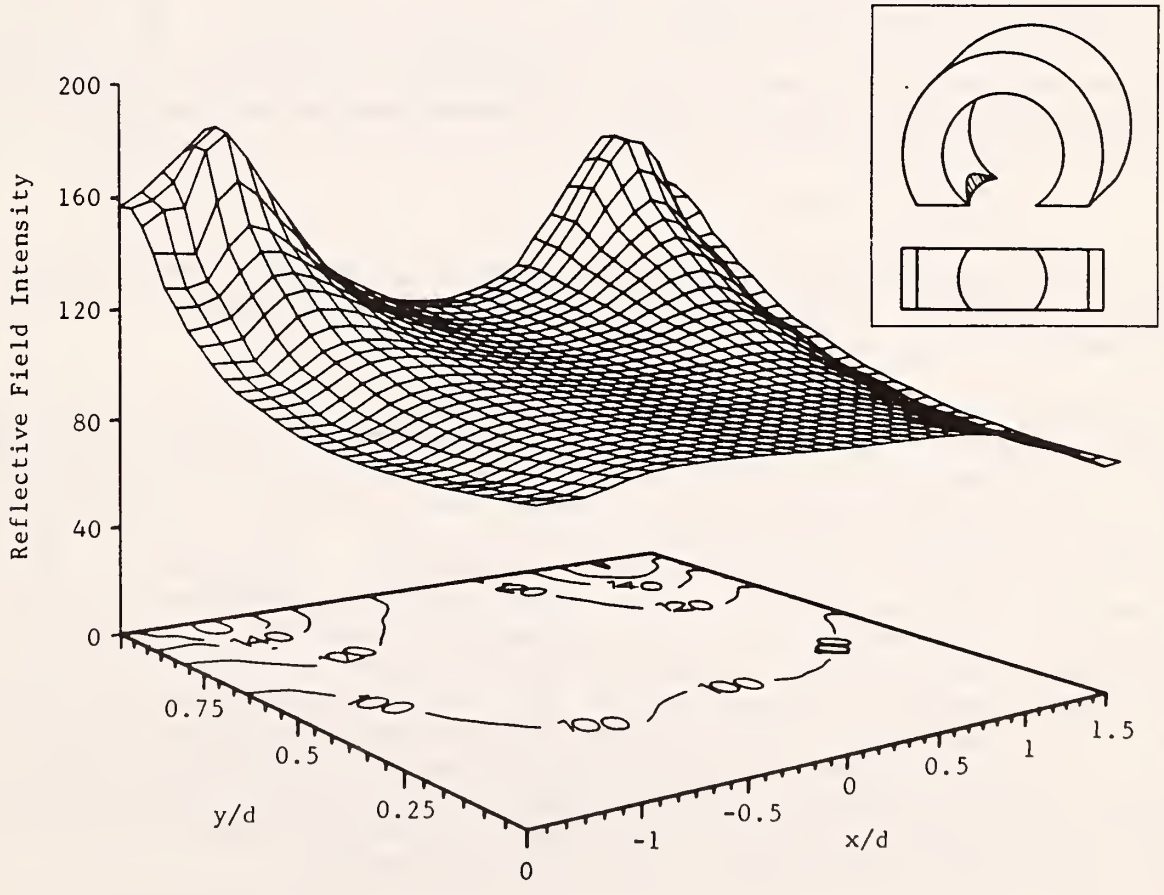

Fig. 6. Two-dimensional maps of the tangential component of the magnetic-field intensity for a uniform-field eddy-current probe fabricated at NBS. The figure shows the field distribution between the two feet of a horseshoe-shape ferrite probe (shown in inset).

The field distribution was mapped in two dimensions with a small probing coil to determine the strength and uniformity of the magnetic field in the active region of the probe. The results of the field mapping, shown in Fig. 6, demonstrate the high degree of uniformity achieved.

We used this new probe to make extensive measurements on simulated and real cracks in titanium alloys to demonstrate the efficacy of the new technique in sizing surface cracks. Typical results obtained from this probe are shown in Fig. 7, where measured flaw signals are compared with predicted flaw signals for a series of five fatigue cracks in Ti-6Al-4V. The cracks were 1 to 1.5 mm long and 0.3 to 0.5 mm deep. Agreement between measured and predicted flaw signals was excellent. A simple inversion procedure was also developed that enabled flaw depths to be determined to within ± 0.1 mm. This probe is being developed for use in the U.S. Air Force's Retirement for Cause Program.

In a related study, we developed new calibration methods suitable for uniform-field eddy-current (UFEC) probes. In calibrating eddy-current probes, the magnetic-field intensity per unit of exciting current, H/I, must be determined, since this quantity enters into any calculation of flaw signals. To calibrate our UFEC probes, we used small cylindrical and spherical recesses machined in the surface of the materials to be studied. The changes in eddy-current probe impedance caused by these recesses were measured and related to the magnetic field strength of the probe by a simple formula:

$$\Delta Z = i(H/I)^2(CV/\sigma\delta^2) \ ,$$

where V is the volume of the recess, δ is the electromagnetic skin depth, σ is the conductivity of the test piece, and C is a shape factor (C = 1 for a cylinder; C = 2 for a sphere).

During the past few years, we have collaborated actively with B. A. Auld of Stanford University in comparing theory and experiment in eddy-current testing. In the past, these studies have focused on typical air-core, absolute, eddy-current probes. This year we extended these studies to a different type of eddy-current probe, the two-port reflection probe. It consists of a drive coil encircling a differential pair of pickup coils. Advantages of reflection probes are very good signal-to-noise ratios and relative insensitivity to variations in the height of the probe above the surface of the workpiece. Theoretical modeling of the probe was carried out at Stanford University, and experimental studies were performed at NBS. We measured signals for a number of rectangular notches in aluminum with a probe constructed at NBS especially for this purpose. The probe construction is illustrated in Fig. 8. We found excellent agreement between theory and experiment, as illustrated in Fig. 9. Extensions of theory to this type of probe are important since they are widely used in industrial and military applications.

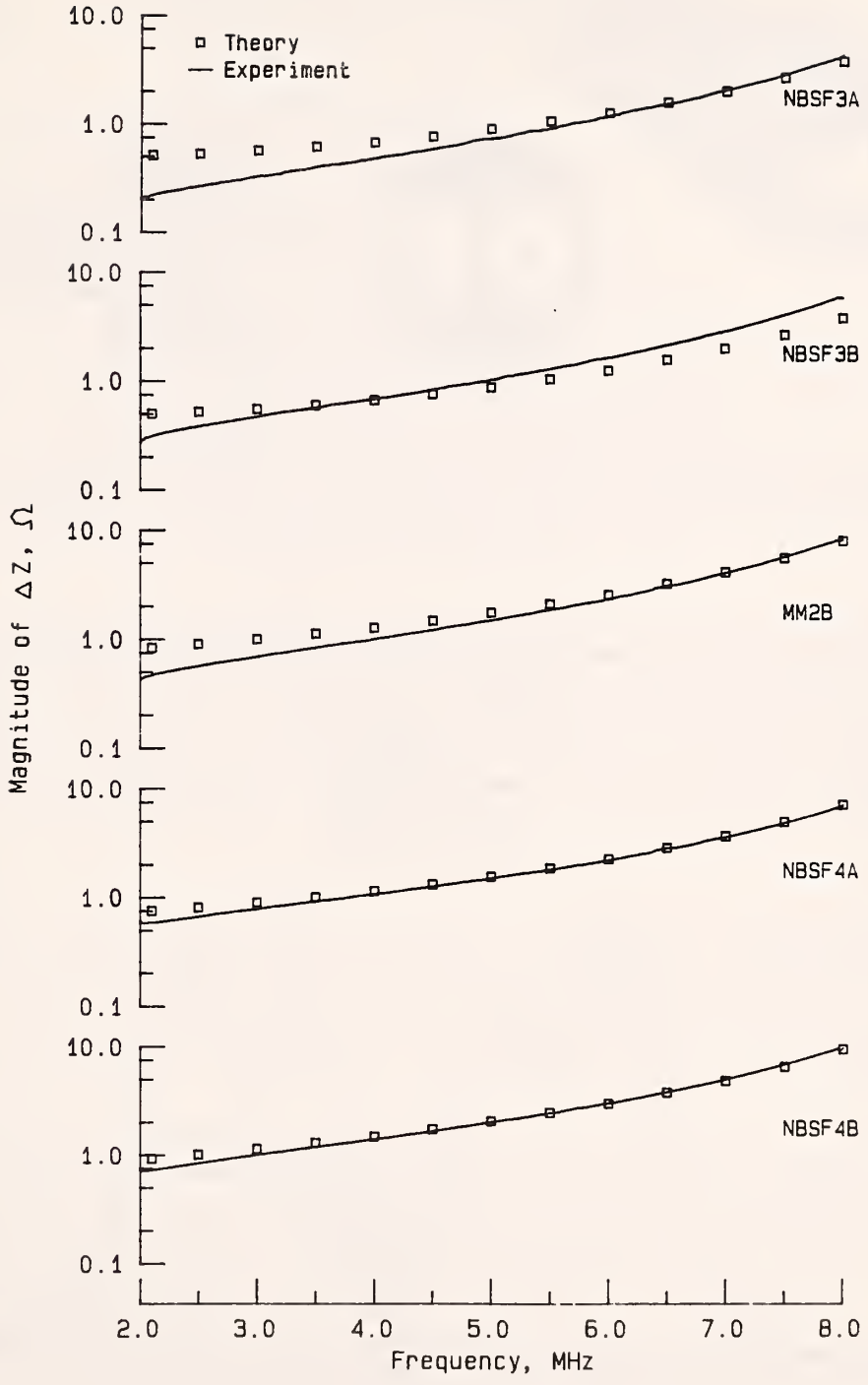

Fig. 7. Results with the uniform-field eddy-current probe.

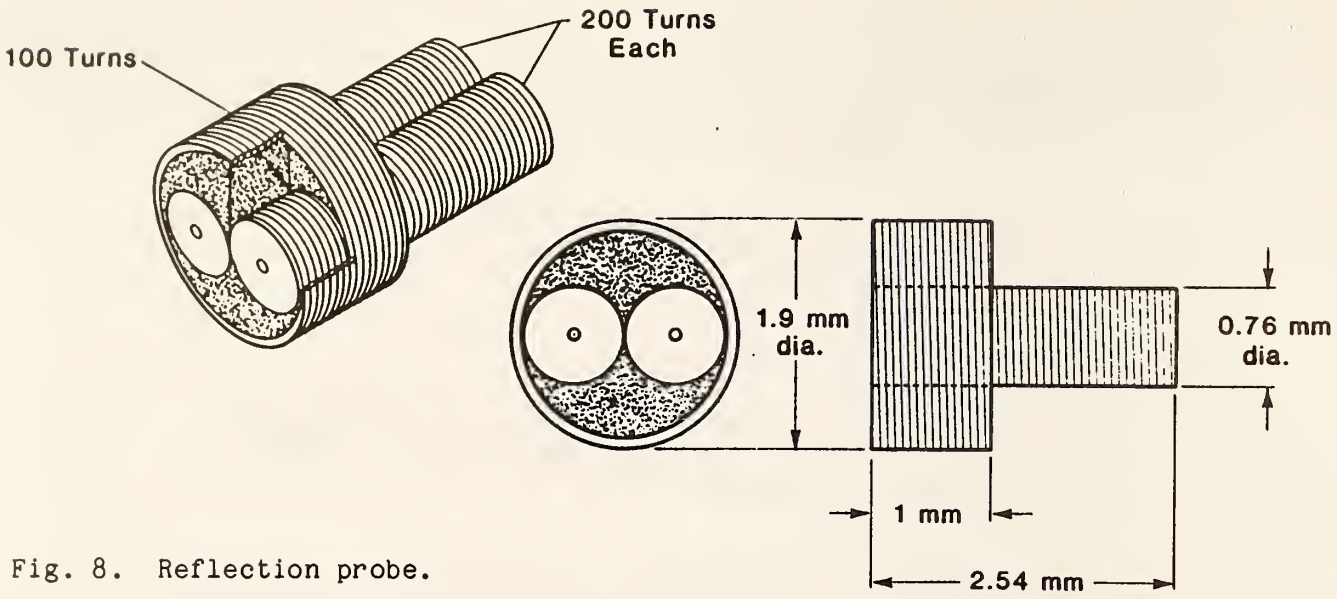

Fig. 8. Reflection probe.

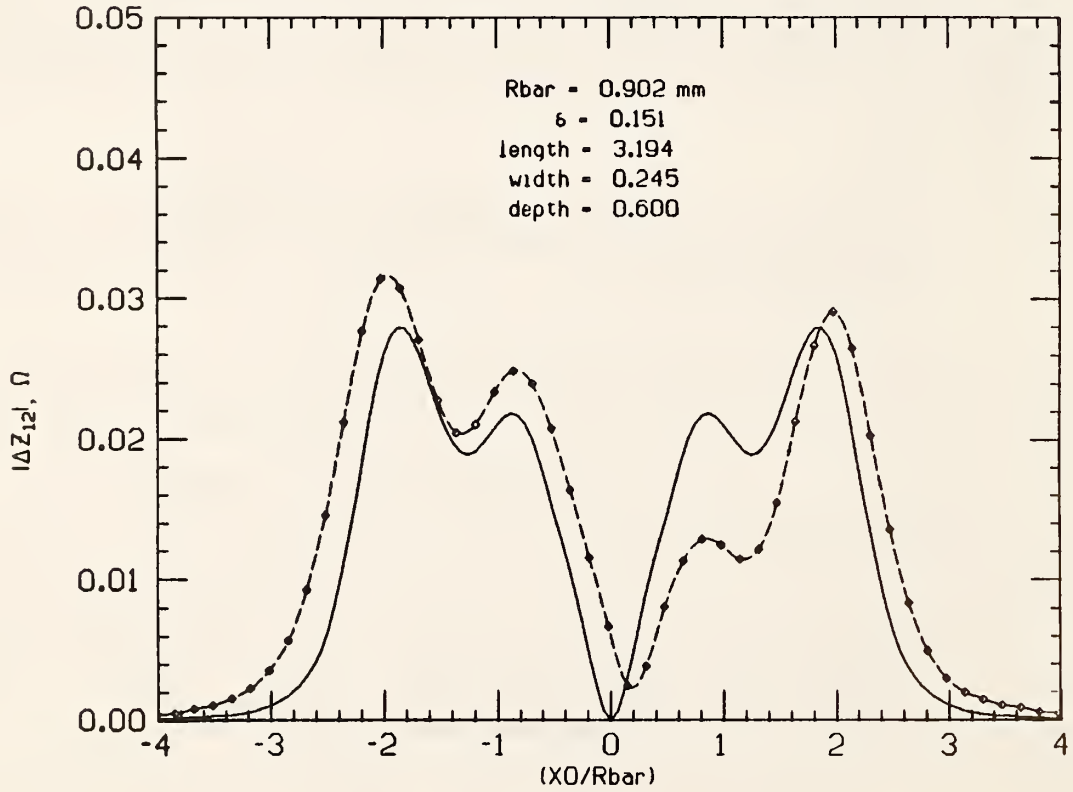

Fig. 9. Results with reflection probe. Dashed line connects experimental values; solid line indicates theoretical values.

Welding

T. A. Siewert, D. Gorni,[1] E. Kivineva,[2] G. Kohn,[3] C. M. McCowan, D. P. Vigliotti

[1]Guest Worker, Armament Development Authority of Israel, Haifa, Israel
[2]Guest Worker, Oulu University, Oulu, Finland
[3]Guest Worker, Nuclear Research Center-Negev, Beer-Sheva, Israel

Welding laboratory

The welding laboratory has been upgraded by the addition of a new control circuit for the transistorized current regulator. The new control circuit expands our capabilities to simulate the static and dynamic response of most power supplies. Our previous control circuit contained three independent adjustments of the power supply response, which enabled simulation of most gas-tungsten-arc power supplies. The new control circuit contains seven independent adjustments of the power supply response; as a result, we can broaden our studies to include gas-metal-arc power supplies, a topic that has been almost ignored in the technical literature.

The current regulator can generate a pure dc waveform by filtering the electrical noise produced in a conventional welding power supply. The pure waveform enables us to study the natural response of welding arcs. A pure waveform is also essential in controlling the penetration of the weld into the plate and, thus, in producing uniform flaws in welds. A series of welds with uniform flaws was produced for the calibration of nondestructive techniques that measure such imperfections.

Arc physics

Our exceptional laboratory facilities (current regulator, laser backlighting system, and high-speed video camera) generate cooperative programs. During the past year, guest scientists from a U.S. university and a national laboratory in Israel have used our laboratory to study droplet transfer in gas-metal-arc (GMA) welding.

During GMA welding, the short-circuit current increases up to the maximum short-circuit current allowed by the controller or up to the point where the liquid metal drop at the end of the electrode detaches and the short circuit is broken. Frames of a high-speed video recording taken at 1/240-s intervals (Fig. 10) show the droplet at the end of the electrode just prior to short circuiting and at detachment.

The current surge that melts the electrode in short-circuiting transfer has been found to continue to increase and result in violent expulsion of the superheated metal as the arc reinitiates. Limiting the maximum current during short circuiting reduces the electromagnetic forces that cause the expulsion; the results are a significant reduction in weld spatter and smooth transfer of the metal to the workpiece.

Fig. 10. Video recording shows portions of the short-circuit welding process: the droplet at the end of the GMA electrode just prior to short circuiting and at detachment. time difference between frames = 1/240 s.

We have improved our understanding of the short-circuiting process: it can be modeled as a period of short circuit, which follows Ohm's law, and a period of stable arc transfer, which can be expressed

$$V = a + bI \quad ,$$

where V is the arc voltage, I is the current, and a and b are experimental constants for each shielding gas mixture and electrode composition. Over time, the stable arc degenerates until a short circuit forms again. This gradual degeneration in the current was modeled by

$$I = I_b + (I_m - I_b)\,[1 - \exp(-t/T_c)] \quad ,$$

where I_b is the stable base current, I_m is the maximum short-circuit current, t is the elapsed time from the end of the short circuiting, and T_c is the power supply time constant.

Evaluation of individual arc reignition events revealed that the variation in the time between these events can be closely correlated with the real-time arc stability. Stable arcs with good weld bead shape and low spatter were found to have very uniform reignition patterns and uniform intervals.

Stainless-steel weldments

We are examining less-common weld compositions and welding processes for a better understanding of why the toughness of stainless steel welds is lower than that of the base metal at cryogenic temperatures. We evaluated electron beam and laser welds in 316LN-type base metal. Both processes have a high completion rate and can join 25-mm plate in one or two passes at relatively high velocity. Fracture toughness tests of compact tension specimens were used to evaluate the weld metal accurately, but their narrow configuration prohibited conventional all-weld-metal tensile tests. Transverse tensile test specimens all broke in the base metal, indicating sufficient strength in the weld. Fracture toughness testing of the weld metal produced $K_{Ic}(J)$ values of 150 to 156 $MPa \cdot m^{1/2}$, only slightly less than the range 159 to 203 $MPa \cdot m^{1/2}$ determined for 316LN-type base metal. We are evaluating a high-nickel (Fe-40Ni-6Cr) shielded-metal-arc (SMA) weld to determine the effect of the nickel on the fracture toughness and strengthening mechanisms at 4 K.

FRACTURE MECHANISMS and ANALYSIS

Our program on fracture mechanisms and analysis has a broad spectrum of goals: (1) the development of fundamental theories on crack-tip structure and processes, (2) the characterization of the mechanical and physical properties related to time-, structure-, and temperature-dependent effects on metals and composites, and (3) the application of established methodologies in the analysis of actual failures.

For structural materials, a knowledge of the fundamentals of crack-tip structures and processes is essential to understanding fracture in these materials and to predicting their long-term service life. Influences of atomic structure and chemical reactions at crack tips have been demonstrated with atomistic models of fracture in a solid, but these influences are only beginning to be confirmed quantitatively by experimental studies of subcritical crack growth and environmental effects. Ductile processes in the high-stress region of the crack tip are being introduced into these atomistic models to assess the role of plastic deformation and to extend the theoretical models to describe crack-growth phenomena, such as creep crack growth and fatigue. High-temperature fracture is a complex process with competitive fracture mechanisms, such as subcritical crack growth, cavity nucleation and growth, and grain-boundary sliding; it is affected by microstructure, impurity content and segregation, processing history, and environment. Failure analysis studies perform a valuable service for those government agencies that have no testing facilities and require research on the safety of structural materials. Using metallographic, x-ray, fractographic, and chemical analysis techniques, our division compiles and analyzes data on many critical structural failures.

Representative Accomplishments

- The elastic fields of dislocation cores and cylindrical inclusions can be represented by line-force defects. The stress concentration at plate-like precipitates can be represented by pileup arrays of these line-force defects. An expression was derived for the thermodynamic force on such a defect produced by stresses acting at its core. The result will be used for treating pileups and other defect interaction problems.

- A transient deformation mechanism map was developed for A36 steel. This diagram, on axes of stress and temperature, tells engineers at a glance the deformation mode (elastic, plastic, or creep) of the most used structural steel. It is particularly useful for assessing the fire resistance of steel structures.

- Two new test techniques have been developed for testing uniaxial filament-reinforced composites: a torsional test method and a method for direct determination of the fracture energy, G_{Ic}, both useful in the 295 to 4 K temperature range. These test methods are the result of a program

to produce optimum components for use in high-technology composite materials. Progress was also achieved in specimen production: high-quality rod-shaped specimens, which require no postproduction machining, are being made under precisely controlled laboratory conditions.

- For graphite-magnesium, a uniaxial fiber-reinforced composite, we ultrasonically measured the complete, nine-component, orthotropic-symmetry, elastic-constant tensor. Using a theoretical model developed previously by us, we successfully modeled these elastic properties. Through inverse modeling, we determined the complete, five-component, hexagonal-symmetry, anisotropic elastic constants for the graphite fiber. By measuring fibers, one can obtain only two of these components.

- Superconducting magnets in fusion energy devices require development of steels with a combination of high strength and high toughness. Toward this goal, we developed provisional equations for the yield strength of AISI 304 and 316 stainless steels at 4 K as a function of nitrogen content and grain size. We also developed provisional equations for the 4-K fracture toughness, $K_{Ic}(J)$, of these alloys, in which the effects of yield strength, nickel and manganese content, and inclusion spacing were assessed quantitatively for the first time. The equations were based on our measurements, which include more extensive numerical data on alloying, refining, and processing parameters than have previously been available.

- A failure analysis was conducted on a pressure vessel that ruptured at an oil refinery and caused a disastrous fire. The steel vessel fractured adjacent to a repair weld along a path that was weakened by hydrogen-induced cracking. Catastrophic fracture occurred at a low stress level (35 MPa) because the toughness of the steel was reduced nearly three-fold by hydrogen embrittlement. Staff of our division directed the investigation; researchers from other divisions and disciplines contributed their expertise. The final report, "Examination of a Pressure Vessel That Ruptured at the Chicago Refinery of the Union Oil Company on July 23, 1984," was delivered to the Occupational Safety and Health Administration.

- We explored technology transfer opportunities in the domestic motor vehicle industry by placing a staff member with the Ford Motor Company for one year. There he gained an understanding of design, testing, and manufacturing procedures and explained the results of the NBS-Battelle studies of annual nationwide costs of fracture and corrosion control that pertain to the motor vehicles and parts sector of the U.S. economy. Recommendations for achieving more efficient use of materials evolved: evaluate the finite-element design codes, develop data bases for mechanical properties of materials, and develop nondestructive evaluation technologies for inspection of as-manufactured parts and real-time manufacturing process control.

Fracture Physics

I.-H. Lin, R. M. Thomson

Research of the Fracture Physics Group is directed toward understanding (1) the toughness or brittleness of materials in terms of their fundamental properties and the interactions between cracks and dislocations and (2) the effects of external chemical environments on cracks in brittle materials.

Over a number of years, we have established a picture of material ductility based on the proposition that material ductility is due, in part, to the atomic configuration of the crack tip and, in part, to the shielding of the crack by external dislocation or other defects. Sharp cracks experience an opening force, which can lead to brittle unstable failure, whereas a wedge or notch experiences no such elastic force and can only grow by ductile processes. A crack is probably sharp only if it is intrinsically stable against dislocation emission. Our work has set criteria for the emission of such dislocations under all sorts of loading conditions at the crack tip in terms of the atomic bonding forces, and we have even looked at the effect of surface stresses on this criterion. Work under way should establish the conditions under which the ductile transition in silicon takes place by means of dislocation emission occurring throughout a zone surrounding the crack tip.

Our recent study shows that externally produced dislocations can have an important effect on the emission criterion because they alter the loading conditions at the tip, and the emission criterion is sensitive to the loading condition. We have work under way that should enable us to test whether these ideas are the foundation of the ductile-brittle transition in body-centered-cubic materials; it should also give us a better feel for the conditions under which the change of shape of the crack caused by the absorption of dislocations can give rise to ductility. With these ideas we hope to be able to understand the formation of "shear cracks" observed in Stage I fatigue and in thin films -- an otherwise puzzling phenomenon.

A crucial part of our analysis involves the shielding provided a crack by dislocations that are generated either externally to the crack or at its tip. In part, this shielding contributes to the overall toughness of the material, but shielding considerations are intimately tied to the emission criteria as well. Our work on shielding has recently been extended to include the effects of grain size and inclusions on the ductile zone. Such effects limit ductile zone size, but there are also direct shielding effects between inclusions and cracks, which are important in composites.

Dynamic and rate effects are needed to determine the ductility of a material. We have recently shown that a critical velocity exists, above which a crack in any material will remain sharp and not emit dislocations. We have begun to study the arrest of fast cracks, which might be produced by some material artifact or loading condition. We suggest that one important factor is the formation of ligaments on the fracture surfaces. Our analysis seems to explain corrosion-induced crack behavior in copper alloys; we are considering extending the study to body-centered-cubic metals. We believe we are beginning to establish the fundamental causes of ductile or brittle behavior in materials.

In our work on chemical effects, we are at a similar watershed. Recently, we have developed a theory of kink generation on sharp cracks in a full-scale, three-dimensional, discrete treatment of the atomic crack structure. In it, we have shown that barriers to crack motion (lattice trapping) are significant only when chemical reactions of a certain kind occur at the tip. A part of this work incorporates a quantum mechanical treatment of the bonds at the crack tip. Although our current work is prototypical in character, it does incorporate the major aspects of any adequate atomic crack theory, and it points the way to more complete treatments in the future. We plan to incorporate the concept of surface forces into our work. These surface forces are the forces exerted by external chemical species on any surface, and in our case, the crack surface. They are long range in nature and thus take place over significant distances near the crack tip. Therefore, they are not easily incorporated into a discrete theory, such as that mentioned above, and must be dealt with by some kind of continuum approximation. We have found extant approaches to this problem (e.g., those based on Barenblatt's theory) inadequate and have developed our own. We are developing an overall theoretical framework that incorporates the discrete effects at the tip with the long-range surface forces. At the same time, we have shown that barriers to crack motion can result from diffusion of chemical species near the tip, and we hope to apply these ideas to recent work on cracks in mica.

Time-Dependent Properties

R. J. Fields, C. H. Brady, M. J. Crooks, R. deWit, D. E. Harne, G. E. Hicho, S. R. Low III, T. R. Shives, L. C. Smith

From the catastrophic failure of a pressure vessel to the creep rupture of 20-year-old steam pipes, the safe and reliable operation of our technological society requires a thorough understanding of the time dependence of mechanical properties. From dynamic to creeping rates, we study the kinetics and kinetic processes behind the mechanical behavior of materials. Although small effects of rate are usually obtained with the normal rate variations applied in the laboratory, ultrahigh rates or creeping rates may give rise to entirely different deformation and fracture behavior. We explore the high-rate regimes by studying the deformation near cracks traveling 500 m/s or more and the effect of strain rates as high as 106/s. We have also developed equipment to generate controlled, high-velocity impacts at 100 to 150 m/s and the instrumentation to monitor material flow and fracture at these high rates. Our work in creep has been mainly at elevated temperatures. In conjunction with AISI, a modeling effort is under way to predict the dominant deformation modes in steel during exposure to a fire.

Transient deformation mechanisms

To ensure the maximum safety of structures that may be exposed to fires, engineers use finite-element techniques to predict the behavior of structural steel. Finite-element codes are an excellent indicator only when they are generated by computer programs that contain sufficient and reliable data for

1. Elastic modulus as a function of temperature
2. Plastic strain as a function of stress and temperature
3. Creep strain as a function of stress, temperature, and time

The total strain for any fire-exposure time, temperature, and stress is the sum of the elastic, plastic, and creep strains.

For such a commercially important steel as A36, considerable data exist on these three types of deformation; however, these data had not been assembled. We have collected as much data as possible, most supplied by the steel industry, and fit the data to appropriate constitutive equations that describe the mechanical behavior as a function of temperature or stress.

Furthermore, the complexity of the finite-element codes depends on whether the predominant mechanical behavior is elastic, plastic, or creep. To determine which mechanisms of deformation appropriately describe a given situation, it is necessary to evaluate and compare the elastic, plastic, and creep equations. We have developed a nomogram that immediately identifies the predominant deformation mechanism for a given stress, temperature, and exposure time. For a given exposure time, the total strain is plotted on stress and temperature axes, as shown in Fig. 1 for A36 steel. By separating regions of one dominant mechanism from another, we have developed a map of

transient deformation mechanisms that is similar to those frequently used for pure metals and a few heat-resistant alloys. This map immediately indicates to the engineer the degree of complexity required in the finite-element code for prediction of structural behavior for a given exposure time in a fire.

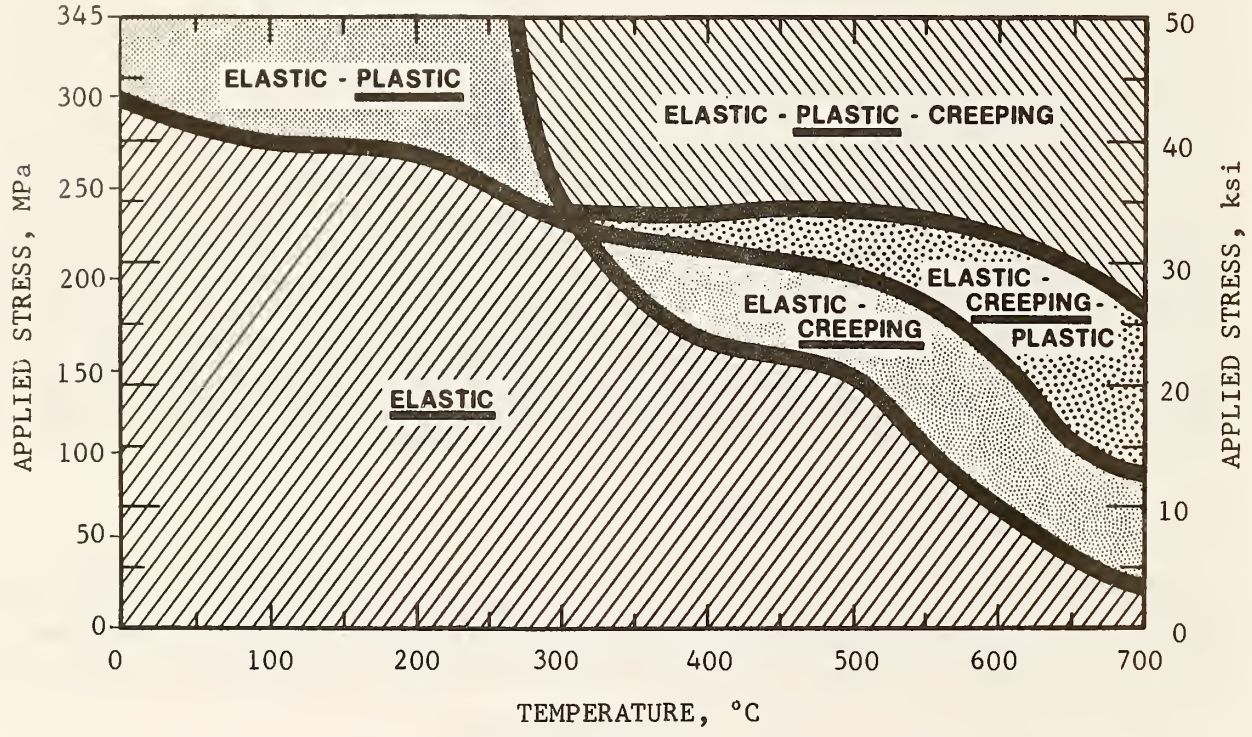

Fig. 1. This transient deformation mechanism map summarizes a large amount of data for the behavior of A36 steel, the steel most commonly used in construction. This particular map shows the deformation mode for a one-hour exposure to a given temperature.

Rate-dependent properties of electrical-grade copper

Copper wires were strained to fracture at rates ranging from 10^{-1} to 10^{3} percent per second. The fracture and deformation properties of the wires were determined as a function of rate and compared with the behavior of a breakaway connector. The Federal Aviation Administration is using this information to assess the need for breakaway electrical connectors in fragile airport lighting structures.

Wide-plate crack-arrest testing

Crack arrest refers to the sudden stopping of a fast fracture. Crack velocities and arrest toughness must be known to prevent disastrous failure of large structures, such as nuclear pressure vessels. We are using new strain-gage techniques and a 53 MN (12 x 10^6 lbf) tensile testing machine to measure these values for some of the largest steel specimens ever tested. Very large specimens are required to avoid intractable complications due to reflected stress waves during the fracture event.

Tests of twenty-two single-edge-crack tensile specimens in a thermal gradient were scheduled between September 1984 and September 1989; eight tests have now been completed. We have obtained crack arrest data at 92°C, the highest temperature at which arrest has been achieved.

Of the four tests completed in the past fiscal year, two were performed on as-received A533B steel and two on a steel that had been heat-treated to simulate radiation embrittlement. Results showed that cleavage fracture could occur at temperatures above the onset of upper-shelf behavior as determined by traditional impact testing. Furthermore, arrest occurred at extraordinarily high values of applied stress-intensity factor.

Composite Mechanics

M. B. Kasen, J. M. Arvidson, M. W. Austin, S. A. Kim, R. D. Kriz, H. M. Ledbetter, M. Lei,[1] L. L. Scull, Y. Shindo[2]

[1]Guest Worker, Institute for Metal Research, Shenyang, P.R. China
[2]Guest Worker, Tohoku University, Sendai, Japan

Substantial effort is directed toward the development and refining of models that will permit accurate prediction of composite material deformation and fracture under a wide variety of conditions. This is particularly important in composite technology where the heterogeneity of the material and the complexity of reinforcement type and distribution precludes the obtaining of such data by experimental means. Primary interest is in understanding damage accumulation mechanisms, factors influencing elastic properties, and parameters influencing residual stress.

Effort is also directed toward understanding the significant parameters influencing mechanical and physical degradation of organic-matrix composites under neutron irradiation at 4 K. These basic data are required in development of functional insulators for superconducting magnets in magnetically confined fusion energy systems. A major effort involves the fabrication and testing of extremely well-characterized research materials.

We also capitalize on our expertise in cryogenic testing of composite and nonmetallic materials by planning and conducting test programs for other agencies, which at the same time contribute to our basic understanding of material performance.

Finite-element modeling of damaged composites

With finite-element models, we studied the influence of various damage states on the behavior of laminated composite materials. We modeled ply cracks and delaminations in both woven and nonwoven laminates. Singularities in stresses near damaged regions or near the stress-free edges were modeled by finite elements to predict the growth of damage. Special elements near regions of stress damage were modeled to include the singular stress field. By analytical methods, we first determined the magnitude of the singularity for the solution of stress distributions near the crack tip. With these singular elements, the complete boundary-value problem for regions far from the crack tip was solved by the finite-element method; the stress-intensity factors were obtained directly and in the same fashion as the nodal displacements.

The influence of residual thermal stresses can be included in the models to study the behavior these materials at low temperatures. For ply cracks terminating at laminated ply interfaces, the conventional stress-intensity factors (Modes I, II, and III) are no longer applicable. The exact physical meaning of the constants obtained by this finite-element method is still under investigation. Nonetheless, the total stress distribution in damaged laminated composites can now be obtained both near these stress singularities and at a distance from them. We will use these models to obtain a better understanding of damage growth in laminated composites.

Screening of composite performance

Ensuring the desired performance of composite materials in many high-technology applications requires optimum selection of the components from which the composite is fabricated. This "component data base" is an essential precursor to the fabrication of engineered composites from which a "design data base" is constructed. Establishing the component data base can be a very lengthy and expensive task owing to the large number of variables that may have to be evaluated. Therefore, we have developed a much more efficient method of performing this work.

We undertook this work when faced with the problem of selecting the optimum components to be used in fabricating fiber-reinforced, organic-matrix materials to be used as insulators in the superconducting magnets of magnetic fusion energy systems. Here, the insulators are subjected to high stress and simultaneously exposed to large fluences of neutron irradiation. Little was known about the significant material properties that control composite performance under such conditons.

Our solution was to develop an efficient, in-house method of producing extremely high-quality specimens in rod form, 3.2 mm in diameter, either unreinforced-resin or uniaxially fiber-reinforced specimens. Complete control is provided over all components and processing. We also developed a series of test methods that can be used with such specimens over the temperature range 295 to 4 K without the requirement of additional machining.

We developed a new method for testing these rods in torsional shear. This is the first time that mechanical testing of composite materials in torsion has been conducted at cryogenic temperatures. In addition to obtaining data on the torsional strength and modulus, with this method we can determine the average adsorbed energy during the deformation and obtain data indicative of the total cracked area developed during the deformation process. We demonstrated that the failure mode in torsion testing of uniaxially reinforced composite specimens occurs primarily at the fiber-matrix interface, as shown in Fig. 2. We also developed a novel method for rapid determination of the fracture energy, G_{Ic}, of the specimens at any temperature (see Fig. 3) and adapted the short-beam shear method for determining apparent interlaminar shear properties to this specimen configuration.

The ease with which these tests can be run, combined with the excellent characterization of the test specimens enables superior composite materials performance screening tests to be performed at a fraction of the cost that would be required if normal procedures were used.

This methodology, developed at NBS, has been accepted internationally as a standard procedure for composite materials development. It is currently being used in Japan in a program being conducted by Osaka University to evaluate composites reinforced with carbon, SiC, and Al_2O_3 fibers.

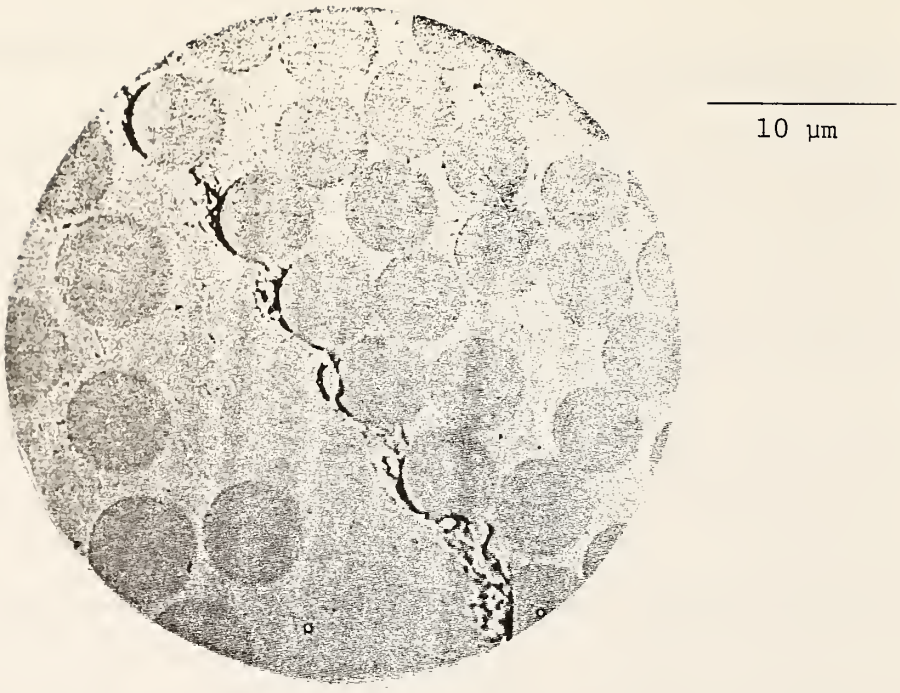

Fig. 2. Appearance of fracture caused by torsion illustrating the interfacial nature of the failure mode.

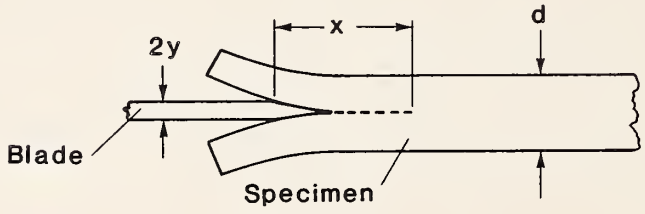

$$G_{Ic} = 0.01372 \frac{d^3 E y^2}{x^4}$$

Fig. 3. Test specimen and equation for determining fracture energy.

Elastic constants

Ultrasonically, we measured the isotropic elastic constants of a tungsten-particle copper-matrix composite. Using scattered-plane-wave, ensemble-average methods, we shall attempt to model the elastic constants.

For graphite-magnesium, a uniaxial fiber-reinforced composite, we ultrasonically measured the complete, nine-component, orthotropic-symmetry, elastic-constant tensor. Using a theoretical model developed previously by us, we successfully modeled these elastic properties. Through inverse modeling, we determined the complete, five-component, hexagonal-symmetry, anisotropic elastic constants for the graphite fiber. By measuring fibers, one can obtain only two of these components.

For a series of uniaxially reinforced glass-epoxy composites, we measured Young's modulus and internal friction by a resonance method. We modeled both properties; for the internal friction, we used a rule-of-mixture damped-oscillator model. Using a computer-controlled inverted torsional pendulum, we determined the internal-friction spectrum between 340 and 4 K in collaboration with M. Weller of the Max Planck Institute in Stuttgart. Characteristic of polymers, the usual α, β, and γ peaks appeared. For both the glass and glass-epoxy interface, an internal-friction peak failed to appear.

We extended our existing composite interface model from zero frequency to finite frequencies. Basically, this model considers the interface as a third phase and predicts the effect of the interface on elastic constants and internal friction (damping). For this model, Y. Shindo of Tohoku University wrote a general computer program.

By x-ray diffraction of SiC_p/Al composites, we determined their internal strain (residual stress) arising from thermal-expansivity mismatch. We found a tensile stress in the matrix that exceeds the non-work-hardened yield strength. Simple modeling supported the observed results. Careful measurements of Young's modulus for these composites indicated several interesting features: anisotropy (caused by processing), a low internal friction (less than 5×10^{-5}), and a linear increase of internal friction with particle volume fraction. Our existing model fails to explain the elastic anisotropy; this question needs further study. The increase in internal friction may arise from interface effects, but we conjecture that it arises from thermal-stress-induced dislocations. The same relationship was observed for fiber volume fraction and internal friction in a study of a SiC_f/Al composite with short fibers aligned partially by mechanical processing. For 25 volume percent of fiber in this composite, the rolling-plane Young's-modulus anisotropy was 15 percent. We intend to model the elastic properties of SiC_f/Al.

Mechanical Metallurgy

G. E. Hicho, J. M. Arvidson, C. H. Brady, M. J. Crooks, R. deWit, R. J. Fields, D. E. Harne, P. T. Purtscher, R. P. Reed, R. Reno, L. L. Scull, T. R. Shives, N. J. Simon, R. L. Tobler, R. P. Walsh

Safe and efficient use of metals and alloys in structural applications requires a thorough data base of mechanical properties. To enlarge this data base, we measure the properties of commercially important metals and alloys. Research ranges from studies on austenitic and high-strength, low-alloy steels to rapidly solidified materials. Properties that are measured and modeled include tensile (flow strength, temperature dependence, activation energy and volume), fatigue (low and high cycle), threshold spectrum loading, crack growth rates, fracture toughness (J-integral, CTOD), shear, bend, and impact. Measurement variables include high and low temperatures, irradiation, and strain rate. In most programs, close collaboration with industry ensures immediate assistance in material development.

In addition to mechanical-property measurement, we study the microstructural origins of these properties. Phase transformations, grain size, dislocation and point defects, solid-solution alloying, inclusions and precipitates, interface behavior, and particle size and aspect ratios all influence the mechanical performance of structural materials. Microstructures are examined by optical and electron metallography. Small-angle neutron scattering (SANS), secondary ion-mass spectrometry, neutron pole figures, Mössbauer spectroscopy, and automated image analysis are used to quantify the microstructure. We alter the microstructure of commercial materials for controlled experiment primarily by heat treatment. Our laboratory capabilities for heat treatment include an austenitizing furnace, two tempering furnaces, a salt pot, and water or oil quenching facilities.

Quantitative metallography

We are developing an automated and standardized means of measuring grain size and shape, and inclusion concentration, size, shape, and distribution. We also intend to obtain these measurements for prototypical lots of steel and use them in quantitative modeling of the effects of processing on microstructure or the effects of microstructure on properties. To date we have automated standardized metallographic preparation, automated quantitative measurements using software we developed, and implemented and tested the Dehoff stereological solution on the NBS computer.

Low-temperature deformation and fracture

Copper and aluminum alloys. The tensile-deformation characteristics and effect of strain rate were studied on relatively pure copper and aluminum alloys, CDA 101 copper and 1100 aluminum. Tensile strain rate was varied by two orders of magnitude (2×10^{-3}; 2×10^{-5} s^{-1}) at temperatures ranging from 295 to 4 K. Tensile stress-strain (for copper, see Fig. 4) and strain-hardening curves (for aluminum, see Fig. 5) were determined for these temperatures. The effect of strain-rate changes on tensile flow strength was measured from strains near 0.002 (yield strength) to more than 0.300.

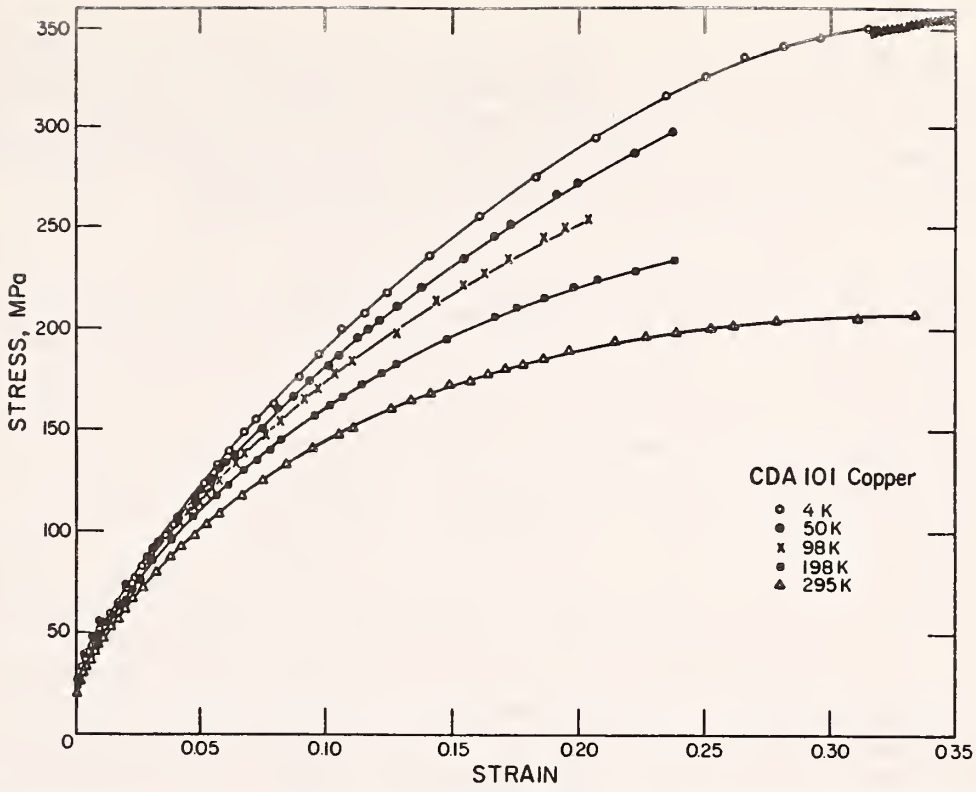

Fig. 4. The tensile stress-strain curves of CDA 101 copper at various temperatures.

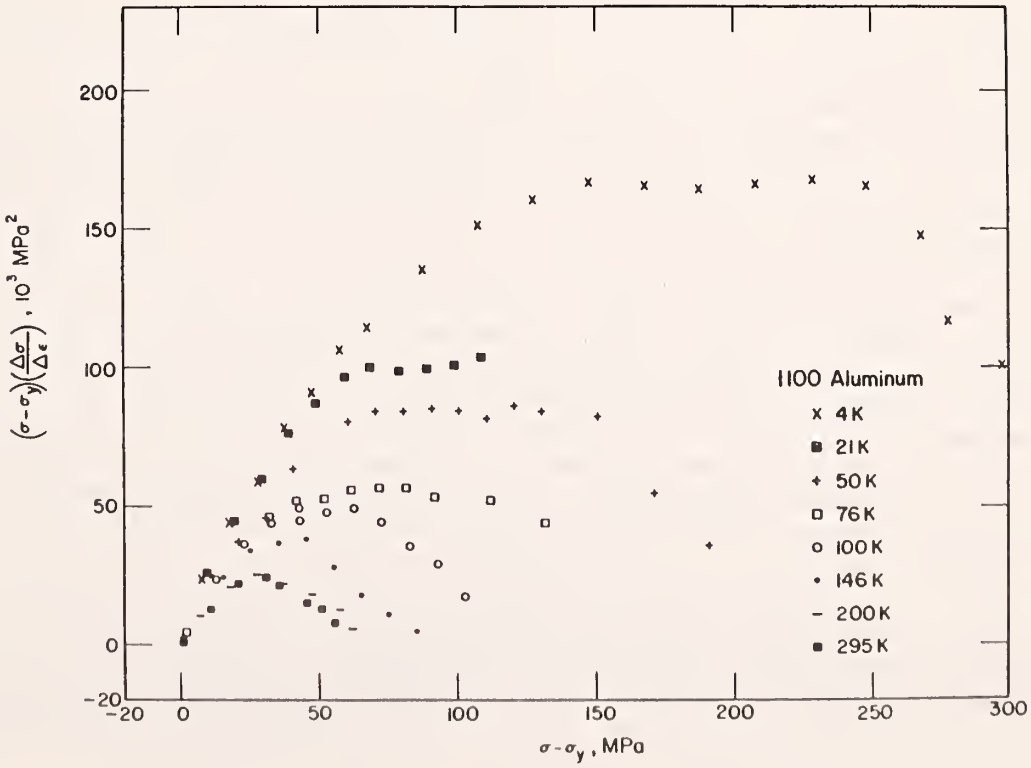

Fig. 5. Strain-hardening characteristics of 1100 aluminum at various temperatures.

The strain-hardening characteristics are best portrayed by using the term $(\sigma - \sigma_y)(d\sigma/d\varepsilon)$ to describe dislocation accumulation as a function of normalized applied stress, $\sigma - \sigma_y$. Two regions are found in copper and aluminum: (1) an athermal, linear range of strong increase of mobile-dislocation density and (2) a range associated with dynamic recovery, where the rate of increase of dislocations levels off and then decreases.

The strain-rate sensitivity characteristics were identified in two ways: (1) as a strain-rate sensitivity parameter, $(\Delta\sigma/\Delta\ell n\dot{\varepsilon})_T$, and (2) as an activation volume, $kT(\Delta\ell n\dot{\varepsilon}/\Delta\sigma)_T$. The strain-rate sensitivity of copper indicates that the frictional stress between dislocations and solute is effectively zero for 99.99 copper, but positive for 99.1 aluminum. This is also indicated in the increased temperature dependence of the yield strength of the aluminum. The effect of solute-dislocation interactions may be reflected in the low-temperature minimum of the activation volume, since it is absent in the copper.

Austenitic stainless steels. The fracture toughness values of twenty-four different compositions of austenitic stainless steels were measured in liquid helium. Three independent factors were found to contribute to the energy required for the initiation of ductile fracture: yield strength at 4 K, substitutional alloying (nickel, manganese, and molybdenum content), and nonmetallic inclusions. Yield strength and inclusions have long been recognized as influencing the toughness of structural alloys and are considered in existing models for fracture toughness. The effects of alloying on the toughness are not directly considered in these models.

The results reaffirm previous results that show toughness decreases with increasing strength. However, at a constant strength level, nickel and possibly manganese and molybdenum significantly increase toughness. This increased toughness is linked to a difference in dislocation interactions and is evidenced by increased plasticity for a triaxial stress state and the transition in fracture morphology. For brittle, faceted fracture, dislocation pileups produce decohesion along slip planes. With higher nickel content, manganese content, or both, dimpled fracture occurs. For the austenitic stainless steels tested, we suggest that the alloy additions increase the stacking-fault energy and make cross slip easier. More cross slip increases plasticity and reduces the stress concentration at the head of dislocation pileups. Then, the preferred site for decohesion would be the interface between inclusions and the matrix. Another factor affecting toughness appears to be the size of dimples produced in ductile fracture. The Ritchie-Thompson model has correctly predicted the trend of decreasing toughness with decreasing dimple size, but the prediction is not quantitative. Problems occur when attempting to correlate the model quantitatively with the test results.

AISI 304- and 316-type alloys. Structural design of superconducting magnets in fusion energy devices requires materials with a combination of high strength and high toughness at 4 K. Nitrogen-strengthened AISI 304 and 316 stainless steels are considered to be the best currently available low temperature structural alloys on the basis of their fabricability and their

potential to meet the U.S. fusion research goals of combined 1000-MPa yield strength and 200-MPa$\cdot m^{1/2}$ fracture toughness at 4 K. Provisional equations for the yield strength of 304- and 316-type alloys at 4 K as a function of nitrogen content and grain size have been developed. Provisional equations for the 4-K fracture toughness, $K_{Ic}(J)$, of these alloys were analyzed, in which the effects of yield strength, nickel and manganese content, and inclusion spacing are expressed quantitatively. The equations resulted from regression analyses of a matrix of NBS measurements that includes more extensive numerical data on alloying, refining, and processing parameters than have previously been available.

Two parameters are most effective in controlling the 4-K strength of 316-type alloys: grain size and nitrogen content. Of these, the variation of nitrogen content is the least expensive. Grain-size control of thick plates requires exceptional rolling capacity. Toughness has been shown to depend on nickel content, inclusion density, and strength. The addition of nickel is rather expensive, and reduction of inclusions demands careful refining practices. Toughness is sacrificed by increasing strength.

Standard test methods. Experimental measurements in support of standard test methods for tensile properties and fracture toughness at temperatures in the liquid helium range are being performed. Effects of variables, such as imposed deformation rates on tensile specimens and disc-groove depth on toughness specimens, need to be documented so that differences of opinion regarding the optimum test method can be resolved. Concurrent measurements are being performed at a group of laboratories in Japan.

Structure and properties of HSLA steels

Our current work on alloy A710 is a culmination of four years of effort to understand the relationship between properties and structure in this HSLA steel. Early work showed that nontraditional heat treatments could raise the yield strength of this alloy to 700 MPa (100 ksi); 550 MPa (80 ksi) is achieved with normal heat treatment. Our most recent research has explored this potential. Through heat treatment, we attained a yield strength of 700 MPa in plates up to 51 mm (2 in.) thick and determined the trade-off in toughness. Using our new microstructural characterization techniques, we determined the heat-induced microstructural changes that were responsible for the changes in properties. We found that Mössbauer spectroscopy together with SANS is a very effective method of studying the retention of austenite during quenching and the kinetics of its transformation during subsequent aging. A new, modified version of A710 is also being studied; it is enriched in alloying elements, particularly nickel and copper, to attain the 700-MPa yield strength without sacrificing toughness. We are providing the U.S. Navy with a data base consisting of the elastic, plastic, and fracture properties of this new alloy measured in tension, compression, and torsion. We are also comparing this new steel with the former A710 alloy to increase our understanding of the role of microstructure in this type of HSLA steel, which may be used in marine structures.

Physical Properties

H. M. Ledbetter, M. W. Austin, S. A. Kim, M. Lei,[1] Y. Shindo[2]

[1]Guest Worker, Institute for Metal Research, Shenyang, P.R. China
[2]Guest Worker, Tohoku University, Sendai, Japan

Physical properties studied by measurement, analysis, and modeling include sound velocities, internal friction, thermal expansivity, specific heat, magnetic susceptibility, volume (mass density), stacking-fault energy, phase transformation, internal strain (residual stress), and especially, elastic constants. We study many types of materials: metals and alloys, polymers, intermetallic compounds, ceramics, and composites, which include particle, fiber, and cloth reinforcement and both metallic and nonmetallic matrices. For most studies, the temperature range is between 295 and 4 K.

Metals

By x-ray diffraction, we determined the stacking-fault energy of several face-centered-cubic metals: copper, gold, nickel, and silver. For manganese, another face-centered-cubic metal, we determined Young's modulus by studying quenched Mn-Cu alloys. Understanding manganese alloying effects in Fe-Cr-Ni austenitic steels depends on knowing this elastic constant. The value determined for Young's modulus, much lower than expected, suggests that gamma manganese is antiferromagnetic. We intend to study this possibility.

Including measurements from 295 to 4 K, we studied the elastic constants of deformed copper. Although the temperature variation showed regular behavior, the ambient-temperature results presented some surprise: low values and symmetry breaking. The texture effect is overwhelmed by a deformation effect. We attribute the loss of $C_{ijkl} = C_{klij}$ symmetry to an anisotropic dislocation array. We believe these dislocations lower Young's modulus by up to ten percent.

Working with B. K. D. Gairola of the University of Stuttgart, we used an elastic-continuum model to predict the polycrystalline quasi-isotropic elastic constants of beryllium. These helped us to interpret the elastic constants we measured on a textured beryllium plate.

Alloys

We determined the elastic constants of a series of Fe-C alloys in collaboration with T. Okamoto of Osaka University. This study led to new elastic-constant values for two of the most important constituents of ferritic steel: pearlite and cementite. The cementite was elastically stiffer and the pearlite softer than anticipated. The soft pearlite, much softer than either cementite or ferrite, suggests a large interface softening.

Between 295 and 4 K, we measured the effect on the elastic constants of alloying molybdenum into Fe-Cr-Ni alloys. Molybdenum, a large and heavy atom, produces large effects: decreased Young's and shear moduli, increased bulk modulus and Poisson's ratio, and decreased paramagnetic-antiferromagnetic (spin-glass) transition temperature. Between 295 and 4 K, we also measured the isotropic elastic constants of a series of Fe-Cr-Ni alloys with manganese added. In both cases, the composition dependence at 295 K approximately paralleled that at 4 K. For one alloy, Fe-13Cr-5Ni-16Mn, we studied other properties -- microstructure, sound velocities, unit-cell size, and magnetic susceptibility; the magnetic transition observed at 181 K clearly shows a low-temperature spin-glass phase.

For a series of binary Ti-Al alloys, we determined the dependence of elastic constants on composition and temperature. Like unalloyed titanium, all these alloys show a shear-modulus anomaly near 50 K. The higher aluminum alloys show another shear-modulus anomaly near 150 K. Young's modulus varies with composition, rising sharply for alloys with more than 12 atomic percent aluminum. We shall attempt to explain these observations theoretically.

Between 295 and 4 K, we measured the isotropic elastic constants of a commercial Al-Li alloy. Our study confirmed a remarkable, unexplained result: lithium increases the Young's modulus of aluminum. Working with T. Suzuki of Tsukuba University and using pseudopotential methods, we calculated the monocrystal elastic constants of Al-Li solid-solution alloys. Our results provide an essential baseline for explaining the remarkable Young's modulus stiffening that lithium produces in aluminum.

For NbC, we measured the monocrystal elastic constants: C_{11}, C_{12}, and C_{44}. Our results suggest a strong ionic-bonding component in the cohesive energy. Properties of the MX compounds (M = transition metal; X = carbon or nitrogen) are essential for a basic understanding of carbon and nitrogen effects on austenitic-steel physical properties.

Measurement methods

In our measurement program, we found a specimen-diameter effect in the usual Marx-oscillator method. Unreported, and unexplained by simple elastic-wave theory, this effect introduced an error of several percent in the $d/D = 0$ limit, where d is the specimen diameter and D is the transducer diameter.

Within our laboratory, we developed a new method to measure Poisson's ratio. Based on odd-harmonic forced vibrations, it provides a useful tool for studying composite-material elastic constants. After further analysis for the anisotropic case, we shall apply the new method to graphite-epoxy composites. We devised a new method to determine the Young's modulus of beryllium; it requires measuring the longitudinal sound velocity and exploring the unusually low Poisson's ratio of beryllium. The method applies to both isotropic and textured aggregates. Compared with usual methods, it requires less time, less effort, and simpler specimens, and it is more accurate.

Working with R. J. Fields of the Mechanical Metallurgy Group, by neutron diffraction we verified a fiber texture in copper rod, a texture predicted by ultrasonic-velocity measurements. Between the two methods, we found close agreement.

Wave propagation

We extended our published theoretical study on waves in orthotropic-symmetry media to waves in monoclinic-symmetry media. Prediction of new wave-propagation phenomena emerged: shear waves that are faster than longitudinal waves and longitudinal-shear mode transitions.

Material Performance

B. W. Christ, C. Brady, A. Choi, M. J. Crooks, R. J. Fields, G. E. Hicho, S. R. Low III, R. P. Reed, T. R. Shives, N. J. Simon

Assessment of the behavior of materials while in service provides valuable insight regarding the ability of models and laboratory tests to predict performance. Other agencies and public utilities bring us materials that have failed for testing and evaluation. We determine the cause of failure and usually recommend ways to prevent such failures. Noteworthy examples of these services are: analysis of the failure of the support structure for an offshore lighthouse (for the Coast Guard); evaluation of tie-down loops on limousines (for the Treasury Department); analysis of the failure of numerous components from coal-fired electricity-generating plants (for a public utility); analysis of the failure of a school bus floor panel and evaluation of the buckling strength of an airplane flap-control rod (for the National Transportation Safety Board). We learn about material problems in service not only from these failure analyses, but also from compilation and review of material performance of specific technologies and conferences and workshops.

Fracture mechanics analysis of a pressure vessel failure

A failure investigation was conducted on a pressure vessel that ruptured at an oil refinery and caused an explosion and fire that killed seventeen people and resulted in extensive property damage. The vessel was an amine absorber tower used to strip hydrogen sulfide from a process stream of propane and butane. The 18.8-m-high, 2.6-m-diameter tank was made of 25-mm-thick plates of ASTM A516 Grade 70 steel in accordance with the ASME Pressure Vessel Code.

The vessel fractured along a circumferential path that was weakened by extensive cracking. These pre-existing cracks initiated in areas of hard microstructure adjacent to a repair weld. The cracks that grew through the vessel wall were caused by hydrogen pressure cracking. When the depth of the largest of these pre-existing cracks exceeded 90 to 95 percent of the wall thickness, leakage occurred because the remaining ligament ruptured. Because the depth of the pre-existing crack was relatively uniform, the thin ligament continued to tear and caused the through crack to grow to a length of about 800 mm.

A fracture mechanics analysis was conducted by using the CTOD fracture criterion to determine if the 800-mm-long crack was sufficient to cause rupture of the vessel at the operating stress level of 35 MPa. The minimum critical CTOD measured was 0.17 mm for specimens notched in the HAZ. The CTOD of the 800-mm-long crack was calculated to be 0.064 mm. Thus, by the CTOD criterion, the crack should have been stable, and sudden rupture should not have occurred. Thus far, however, a key feature of the vessel's condition had not been accounted for: the steel plates had been charged with hydrogen, as indicated by the presence of blisters, delaminations, and hydrogen-induced cracking in these plates. Therefore, additional fracture toughness tests were conducted on steel samples notched in the HAZ and charged with hydrogen. The measured CTOD values ranged from 0.064 to 0.096 mm. The agreement

Table 1. Reducible Costs* for Cars, Buses, Trucks, and Their Parts

Sellers \ Buyers		INDUSTRIES			TOTAL DOMESTIC OUTPUT	FINAL DEMAND						TOTAL INCOME FROM OUTPUTS
			Cars, Buses and Trucks			Personal Consumption	Capital Purchases	Export	Government Purchases	Other	Total Final Demand	
COMMODITIES												
	Cars, Buses, and Trucks		-636.6		-1039	-144.1	-216.9	0	-36.7	-0.1	-398	-1437
TOTAL DOMESTIC INPUT			-3618									
SOCIAL SAVINGS (increased profit)			+2682									
DOMESTIC VALUE ADDED	Labor											
	Profit											
	Taxes											
	Interest											
	Other											
	Total Dom. Value Added		-278.7									
OTHER	Imports		-222.6									
TOTAL VALUE ADDED			-501									
TOTAL EXPENDITURES FOR INPUTS			-1437									

*Differences between the actual 1978 economy and the hypothetical 1978 economy of best fracture control practices in millions of 1978 dollars; totals are rounded to the nearest million. Table is from "Assessing Technology Transfer Opportunities Beneficial to the Domestic Motor Vehicle Industry," B. W. Christ and R. W. Landgraf, NBS Special Publication, to be published. Data are from Appendix H of "Final Report on Economic Effects of Fracture in the United States," submitted to the National Bureau of Standards in September 1982 by Battelle-Columbus Division, Columbus, Ohio.

between these measured values and the calculated CTOD indicates that fracture of the vessel was possible at a stress level of 35 MPa for an 800-mm-long crack because the toughness of the steel was reduced by hydrogen embrittlement.

Assessment of technology transfer opportunities beneficial to the domestic motor vehicle industry

A staff member spent one year with the Ford Motor Company to explore technology transfer opportunities in the domestic motor vehicle industry by developing relationships with engineers and policymakers in the industry and obaining an understanding of design, testing, and manufacturing procedures. He explained results of the NBS-Battelle studies of annual nationwide costs of fracture control (1978) and corrosion control (1975), which pertain to the motor vehicles and parts sector of the U.S. economy.

Annual reducible fracture control costs in this sector alone were estimated to be about $3 billion, which is the sum of the Final Demand and Social Savings figures in Table 1. More efficient use of materials through reduction in size, integration of parts, and increased design efficiency could lead to the substantial reductions for structural material costs shown in Table 2. The associated weight reduction is a secondary benefit, reducing fuel consumption in accord with the government policy of Corporate Average Fuel Economy. Some reduction in vehicle size has occurred since 1976, as shown in Fig. 6. Experts throughout the automotive industry feel that integration of steel parts is an engineering activity worthy of much more attention than it is now receiving.

More efficient use of structural materials in design is being addressed by such techniques of modern technology as computer-assisted service-load measurements, finite-element stress analysis (see example in Fig. 7), and computer models for fatigue lifetime prediction. To refine the efficiency of designs, the precision of various finite-element codes used by designers needs to be evaluated. For maximum design efficiency, data-base development for mechanical properties is needed to provide designers with accurate data on the magnitude and variability of properties. Also, nondestructive evaluation technologies must be developed for inspection of as-manufactured parts and real-time manufacturing process control.

Table 2. Estimated Reducible Costs through Efficient Use of Materials

Material	Reducible Cost (millions of 1978 dollars)
Iron and carbon steel	1894.4
Aluminum alloys	229.7
Other nonferrous metals	106.1
Alloy steel	79.8
Stainless steel	19.9

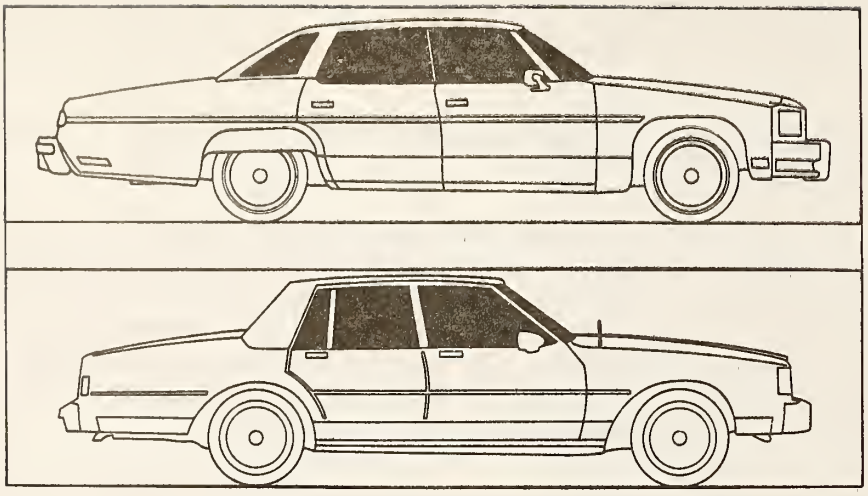

Fig. 6. The trend toward production of smaller, lighter automobiles in the United States is illustrated by the profiles of one model in 1976 (a) and in 1986 (b). Weight was saved by more efficient use of materials, substitution of lighter, stronger materials, and changes in design. (Courtesy of Scientific American.)

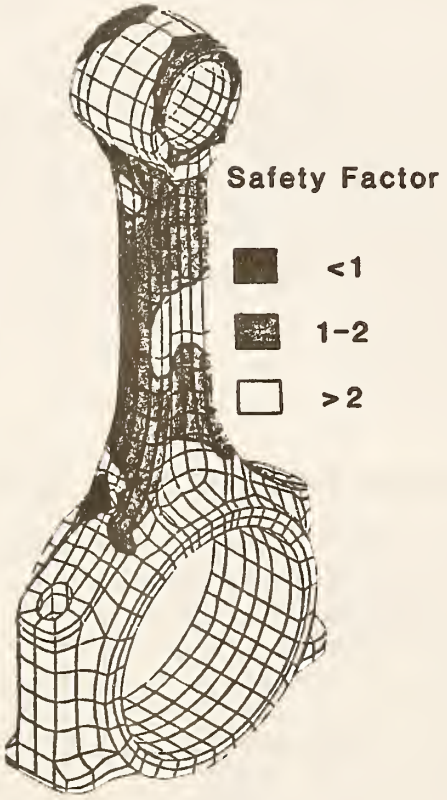

Fig. 7. Finite-element analysis of a connecting rod.

Montana pipeline

At the request of the Office of Pipeline Safety of the U.S. Department of Transportation and the Montana Public Service Commission in March 1984, staff of our division have provided technical assistance in the evaluation of a natural gas transmission pipeline built in 1983 for the Montana Power Company of Butte, Montana. Construction of this 160-km (100-mi.) underground pipeline was according to the Code of Federal Regulation, Title 49, Part 192. We provided technical assistance at public hearings and at construction sites in Montana in matters related to interpretation and application of the Federal pipeline regulations, and stability of the pipeline in the ground, pipeline corrosion protection, and stability of cracks in girth welds. We have begun a three-year program of nondestructive-evaluation monitoring of the approved pipeline. A fracture mechanics analysis of girth-weld cracks by our staff indicated that 30 of these cracks that were 25 mm (1 in.) in length or less could be safely left in this pipeline. This analysis was based on our previous analytical work on the Alaska Oil Pipeline, experimental results by Battelle-Columbus from pipeline burst tests conducted for the American Iron and Steel Institute, and experimental results by Southwest Research Institute on segments of the Montana pipeline.

The NBS technical consultation was instrumental in the granting of a Final Order of Approval of this pipeline by the Montana Public Service Commission and the Office of Pipeline Safety in August 1986. Incorporated in this order is the first waiver of the requirement in CFR 49, Part 192 that girth-weld cracks in natural gas transmission pipelines be completely removed.

Materials evaluation for railroad applications

Our research for the U.S. railroad industry has three aspects: (1) understanding the causes of material behavior that have contributed to accidents, (2) providing complete and current data bases for mechanical properties of materials traditionally used by the rail industry, and (3) evaluating new materials and NDE tools for the rail industry.

Rail failures, wheel failures, and tank-car punctures are examples of the problems encountered by the rail industry. These failed components are brought to NBS for further testing and evaluation to understand the causes of their failures and how they might be avoided in the future. In the past year, a study on the unfractured mate to a fractured wheel included hardness testing, metallographic examination, and determination of residual stress. The J-integral testing procedure was used to determine the toughness of steel from a punctured tank car, which, in service, had been exposed to nitric acid and other hazardous chemicals that are incompatible with steel.

The suitability of these materials for use in the rail industry has usually not been evaluated in terms of their material properties. Research has been directed at measuring the plastic and fracture properties (as a function of temperature and loading rate) of an aluminum alloy that is commonly used in railroad tank-car shells. In collaboration with the Nondestructive Evaluation Group within our division, we have made a considerable effort to develop

a noncontacting means of determining the residual stress state of railroad wheels. This information, together with a fracture-toughness data base, provides an estimate of critical flaw size in wheels. Substantial progress has been made in the use of EMATs for this purpose.

Standard reference materials

Two standard reference materials are produced: ferrite-austenite standards and electrical conductivity standards. The ferrite-austenite standards are produced to assist industry in the determination of retained austenite in ferrite and retained δ-ferrite in austenite, particularly welds. Since the retained component is usually deleterious to mechanical properties, it is important to limit the amount retained. These standards are made by a powder processing route and validated by automated image analyses and x-ray fluorescence techniques. The electrical conductivity standards provide readily transferable reference standards for 30 and 40 percent IACS. These standards are used primarily for the calibration of eddy-current gages, which are used routinely in industry for nondestructive detection of cracks, preferential thinning, and other flaws in metallic components. Therefore, these standards are useful in determining structural reliability. They are produced from high-purity copper-based alloys that are forged and annealed to generate an extremely uniform microstructure.

Evaluation of all marketed hardness standards is another project under way. In conjunction with ASTM, hardness testers have been consigned to NBS and hardness test blocks and indentors have been supplied by U.S. industry. The first step, choosing a set of prototypical diamond-cone indentors, has been completed. This step employed interferograms and actual penetration behavior in single-crystalline material as evaluative methods. Using these indentors and the consigned testing machines, in the next fiscal year we will make a comparative study of all hardness standards marketed in the United States.

Material properties handbook

The Materials Handbook for Fusion Energy Systems (MHFES) is being developed to provide an authoritative common source of material properties for the fusion energy community to use in concept evaluation, design, safety analysis, and performance prediction and verification of fusion energy systems. This single source for properties is essential to ensure a common basis for comparing the eventual performance and economics of the various fusion systems currently under study, in operation, or under construction.

Handbook pages have been provided to the MHFES covering low-temperature properties of structural alloys for the superconducting magnets used for plasma confinement in fusion energy devices. Three nitrogen-strengthened austenitic stainless steels that are the most promising near-term candidates for structural use in superconducting magnets were chosen for initial coverage. Initial work for preparation of handbook pages on aluminum alloys has been completed. Current work involves a review of properties of several high-purity coppers and copper alloys: CDA 101, 102, 104, 105, 107, 155, and 170 through 175.

OUTPUTS
and
INTERACTIONS

SELECTED RECENT PUBLICATIONS

Auld, B. A.; Jefferies, S.; Moulder, J. C.; Gerlitz, J. C. Semi-elliptical surface flaw EC interaction and inversion: theory. Thompson, D. O.; Chimenti, D. E., eds. Review of Progress in Quantitative Nondestructive Evaluation, vol. 5A. New York: Plenum; 1986. 383-393.

Arvidson, J. M.; Scull, L. L. Compressive properties of silica aerogel at 295, 76, and 20 K. Reed, R. P.; Clark, A. F., eds. Advances in Cryogenic Engineering--Materials, vol. 32. New York: Plenum; 1986. 243-250.

Capobianco, T. E.; Fickett, F. R.; Moulder, J. C. Mapping of eddy current probe fields. Thompson, D. O.; Chimenti, D. E., eds. Review of Progress in Quantitative Nondestructive Evaluation, vol. 5A. New York: Plenum; 1986. 705-711.

Capobianco, T. E.; Moulder, J. C.; Fickett, F. R. Flaw detection with a magnetic field gradiometer. Moore, D. W.; Matzkanin, G. A., eds. Proceedings of the 15th Symposium on Nondestructive Evaluation. San Antonio: NTIAC; 1986. 15-20.

Cardenas-Garcia, J. F.; Read, D. T.; Moulder, J. C. Experimental study of the J-integral in an aluminum tensile panel. Proceedings of the 1986 SEM Spring Conference on Experimental Mechanics. Bethel, Connecticut: Society for Experimental Mechanics; 1986. 448-457.

Christ, B. W. Failure analysis: nondestructive evaluation. Bever, M. B., ed. Encyclopedia of Materials Science and Engineering. Oxford: Pergamon; 1986. 1617-1619.

Clark, A. V., Jr.; Fukuoka, H.; Mitraković, D. V.; Moulder, J. C. Characterization of residual stress and texture in cast steel railroad wheels. Ultrasonics 24: 281-288; 1986.

Clark, A. V., Jr.; Moulder, J. C. Measurement of residual stresses in slightly anisotropic aluminum alloy specimens by the method of acoustic birefringence. Ultrasonics. In press.

Clark, A. V., Jr.; Moulder, J. C. Absolute ultrasonic determination of stresses in aluminum alloys. Thompson, D. O.; Chimenti, D. E., eds. Review of Progress in Quantitative Nondestructive Evaluation, vol. 5B. New York: Plenum; 1986. 1449-1459.

Clark, A. V., Jr.; Moulder, J. C.; DelSanto, P. P.; Mignogna, R. B. A comparison of several ultrasonic techniques for absolute stress determination in the presence of texture. Achenbach, J. D.; Rajapakse, Y., eds. Symposium on Solid Mechanics Research for Quantitative NDE. The Hague: Martinus Nijhoff; 1986. In press.

Clark, A. V., Jr.; Moulder, J. C.; Trevisan, R. E.; Siewert, T. A.; Mignogna, R. B. Ultrasonic techniques for residual stress measurement in thin welded aluminum alloy plates. Thompson, D. O.; Chimenti, D. E., eds. Review of Progress in Quantitative Nondestructive Evaluation, vol. 5B. New York: Plenum; 1986. 1461-1472.

Danko, G. A.; Low S. R., III; deWit, R.; and Fields, R. J. Wide plate crack arrest testing: instrumentation for dynamic strain measurements. Shives, R. T., ed. Use of New Technologies to Improve Mechanical Readiness, Reliability, and Maintainability. Proceedings of the 40th Meeting of the Mechanical Failures Prevention Group. Cambridge, U.K.: Cambridge University Press. In press.

Datta, S. K.; Ledbetter, H. M. Effect of interface properties on wave propagation in a medium with inclusions. Selvadurai, A. P. S.; Voyiadjis, G. Z., eds. Mechanics of Material Interfaces. Amsterdam: Elsevier; 1986. 131-142.

Datta, S. K.; Ledbetter, H. M. Interface effects on attenuation and phase velocity in metal-matrix composites. Thompson, D. O.; Chimenti, D. E., eds. Review of Progress in Quantitative Nondestructive Evaluation, vol. 6. New York: Plenum. In press.

Datta, S. K.; Ledbetter, H. M. Ultrasonic characterization of material properties of composite materials. Proceedings, Tenth U.S. National Conference on Applied Mechanics. New York: American Society of Mechanical Engineers. In press.

Datta, S. K.; Ledbetter, H. M. Ultrasonic-velocity studies in metal-matrix composites: measurements and modeling. Proceedings, Nondestructive Testing and Evaluation of Advanced Materials and Composites Conference. San Antonio, Texas: Nondestructive Testing Information Analysis Center; Santa Barbara, California: Metal Matrix Composites Information Analysis Center; Columbus, Ohio: Metals and Ceramics Information Center. In press.

Datta, S. K.; Shah, A. H.; Ledbetter, H. M. Ultrasonic scattering and NDE of materials and cracks. Proceedings, ONR Symposium on Solid Mechanics Research for Quantitative NDE. The Hague: Martinus Nijhoff; 1986. In press.

DelSanto, P. P.; Mignogna, R. B.; Clark, A. V., Jr. Ultrasonic texture analysis for polycrystalline aggregates of cubic materials displaying orthotropic symmetry. Ruud, C. O.; Green, R. E., eds. Proceedings of the 2nd International Symposium on Nondestructive Characteristics of Materials. New York: Plenum. In press.

deWit, R. Appendix: K-R Curve with Dugdale model. Newman, J. C., Jr.; Loss, F. J., eds. An Evaluation of Fracture Analysis Methods. Philadelphia: American Society for Testing and Materials; 1985. 79-83.

deWit, R.; Fields, R. J. Wide plate crack arrest testing. Nucl. Eng. Des. In press.

Early, J. G.; Shives, T. R.; and Smith, J. H. Failure Mechanisms in High Performance Materials; Proceedings of the 39th Meeting of the Mechanical Failures Prevention Group. Cambridge, U.K.: Cambridge University Press; 1985. 234 pp.

Fields, R. J.; Dobbyn, R. D.; Glinka, C. I. Microstructural characterization by small angle neutron scattering. Wadley, H. N. G., ed. Nondestructive Evaluation of Microstructure for Process Control. Metals Park, Ohio: American Society for Metals; 1986. 123-131.

Grong, O.; Siewert, T. A.; Edwards, G. R. Effects of deoxidation practice on the transformation behavior and toughness of steel welds. Weld J. In press.

Grong, O.; Siewert, T. A.; Martins, G. P.; Olson, D. L. A model for the silicon-manganese deoxidation of steel weld metals. Metall. Trans. In press.

Hicho, G. E.; Brady, C. H.; Smith, L. C.; Fields, R. J. Effect of heat treatment on the mechanical properties and microstructures of four different heats of ASTM A710 steel. J. Heat Treat. In press.

Hirth, J. P.; Lin, I.-H. The thermodynamic force on line force defects. Philos. Mag. A. In press.

Jones, E. R., Jr.; Datta, T.; Almasan, C.; Edwards, D; Ledbetter, H. M. Low-temperature magnetic properties of fcc Fe-Cr-Ni alloys: Effects of manganese and interstitial carbon and nitrogen. Mater. Sci. Eng. In press.

Kasen, M. B. An alternative view of diffusion-induced grain boundary motion. Philos. Mag. A 54(1): L31-L35; 1986.

Kasen, M. B. Development of radiation-resistant organic insulators for magnetic fusion energy applications. Goel, V. S., ed. Nuclear Power Plant Aging, Availability Factor and Reliability Analysis. Metals Park, Ohio: American Society for Metals; 1985. 265-268.

Kasen, M. B. High quality organic matrix composite specimens for research purposes. Compos. Technol. Rev. In press.

Kasen, M. B. Standardizing nonmetallic composite materials for cryogenic applications. Seminar on Property Evaluation and Standardization of Cryogenic Materials (Preliminary Publication). Tokyo: Cryogenic Engineering Society of Japan; 1986. 1-6.

Kasen, M. B. Strategy for the data base construction of radiation-resistant cryogenic composite insulators for magnetic fusion energy applications. Proceedings, International Symposium on Fundamental Research Strategy in the Development of New Materials for Efficient Energy Conversion. Osaka, Japan: ISIR Osaka University; 1986. 112-117.

Kasen, M. B.; Hicho, G. E. Handling blunt flaws in a fitness-for-service assessment of pipeline weld quality. Goel, V. S., ed. The Mechanism of Fracture. Metals Park, Ohio: American Society for Metals; 1986. 295-304.

Kasen, M. B.; Stoddard, R. B. Screening the performance of organic insulators under cryogenic irradiation. Reed, R. P.; Clark, A. F., eds. Advances in Cryogenic Engineering--Materials, vol. 32. New York: Plenum; 1986. 153-159.

Kohn, G.; Siewert, T. A. The effect of power supply response characteristics on droplet transfer of GMA welds. Proceedings, ASM International Conference on Trends in Welding Research. Metals Park, Ohio: American Society for Metals. In press.

Kriz, R. D. Edge stresses in woven laminates at low temperatures. Proceedings, Ninth ASTM Symposium on Composite Materials: Fatigue and Fracture. Philadelphia: American Society for Testing and Materials. In press.

Kriz, R. D.; Ledbetter, H. M. Elastic representation surfaces of unidirectional graphite-magnesium. Proceedings, Nondestructive Testing and Evaluation of Advanced Materials and Composites Conference. San Antonio, Texas: Nondestructive Testing Information Analysis Center; Santa Barbara, California: Metal Matrix Composites Information Analysis Center; Columbus, Ohio: Metals and Ceramics Information Center. In press.

Kriz, R. D.; Muster, W. J. Influence of damage on mechanical performance of woven laminates at low temperatures. Reed, R. P.; Clark, A. F. eds. Advances in Cryogenic Engineering--Materials, vol. 32. New York: Plenum; 1986. 137-144.

Ledbetter, H. M. Low-temperature sound velocities in 304-type stainless steels: effect of interstitial C and N. Res Mech. 18: 245-250; 1986.

Ledbetter, H. M.; Austin, M. W. Internal strain (stress) in an SiC/Al particle-reinforced composite. Barrett, C. S.; Cohen, J. B.; Faber, J., Jr.; Jenkins, R.; Leyden, D. E.; Russ, J. C.; Predecki, P. K., eds. Advances in X-Ray Analysis, vol. 29. New York: Plenum; 1986. 71-78.

Ledbetter, H. M.; Austin, M. W. Internal strain (stress) in an SiC/Al particle-reinforced composite: an x-ray diffraction study. Mater. Sci. Eng. In press.

Ledbetter, H. M.; Austin, M. W.; Kim, S. A. Carbon and nitrogen effects on the elastic constants of AISI type 304 stainless steel at 4 K. Mater. Sci. Eng. In press.

Ledbetter, H. M.; Chevacharoenkul, S.; Davis, R. F. Monocrystal elastic constants of NbC. J. Appl. Phys. 60: 1614-1617; 1986.

Ledbetter, H. M.; Datta, S. K. Effective wave speeds in an SiC-particle-reinforced Al composite. J. Acoust. Soc. Amer. 79: 239-248; 1986.

Ledbetter, H. M.; Lei, M.; Austin, M. W. Young modulus and internal friction of a fiber-reinforced composite. J. Appl. Phys. 59: 1972-1976; 1986.

Lin, I.-H.; Thomson, R. Cleavage, dislocation emission, and shielding for cracks under general loading. Acta. Metall. 34(2): 187-206; 1986.

Lin, I.-H. Macrocrack-dislocation pileup interactions. Mater. Sci. Eng. 81: 325-335; 1986.

Lin, I.-H.; Thomson, R. M. Dynamic cleavage in ductile materials. J. Mater. Res. 1(1): 73-80; 1986.

Lin, I.-H.; Thomson, R. M. The influence of dislocation density on the ductile-brittle transition in bcc metals. Scr. Metall. In press.

McCowan, C. N.; Siewert, T. A.; Tobler, R. L. Tensile and Fracture properties of an Fe-18Cr-20Ni-0.16N fully austenitic weld metal at 4 K. J. Eng. Mater. Technol. In press.

McHenry, H. I. Metals and alloys for low temperatures. Handbook of Applied Thermal Design. New York: McGraw-Hill. In press.

McHenry, H. I.; Shives, T. R.; Read, D. T.; McColskey, J. D.; Brady, C. H.; Purtscher, P. T. Examination of a Pressure Vessel that Ruptured at the Chicago Refinery of the Union Oil Company on July 23, 1984. Nat. Bur. Stand. (U.S.) NBSIR 86-3049; 1986 March. 218 pp.

Moulder, J. C.; Capobianco, T. E. Detection and sizing of surface flaws with a SQUID-based eddy current probe. J. Res. Natl. Bur. Stand. In press.

Moulder, J. C.; Gerlitz, J. C., Auld, B. A.; Jefferies, S. Semi-elliptical surface flaw EC interaction and inversion: experiment. Thompson, D. O.; Chimenti, D. E., eds. Review of Progress in Quantitative Nondestructive Evaluation, vol. 5A. New York: Plenum; 1986. 395-402.

Moulder, J. C.; Read, D. T.; Cardenas-Garcia, J. F. A new video-optical method for whole-field strain measurements. Proceedings of the 1986 SEM Spring Conference on Experimental Mechanics. Bethel, Connecticut: Society for Experimental Mechanics; 1986. 700-705.

Read, D. T. Fracture mechanics analysis and critical flaw size curves for surface flaws in pipelines. Goel, V. S., ed. The Mechanism of Fracture Metals Park, Ohio: American Society for Metals; 1986. 561-568.

Read, D. T.; Moulder, J. C.; Cardenas-Garcia, J. F. Experimental study of path independence of the J-integral in an HSLA steel tensile panel. Van Elst, H. C.; Bakker, A., eds. ECFG: Fracture Control of Engineering Structures, vol. I. Warley, U.K.: Engineering Materials Advisory Services; 1986. 395-413.

Reed, R. P., ed. Materials Studies for Magnetic Fusion Energy Applications at Low Temperatures--IX. Nat. Bur. Stand. (U.S.) NBSIR 86-3050; 1986 May. 338 pp.

Reed, R. P.; Clark, A. F., eds. Advances in Cryogenic Engineering--Materials, vol. 32. New York: Plenum; 1986. 1120 pp.

Reed, R. P.; Purtscher, P. T.; Yushchenko, K. A. Nickel and nitrogen alloying effects on the strength and toughness of austenitic steels at 4 K. Reed, R. P.; Clark, A. F., eds. Advances in Cryogenic Engineering--Materials, vol. 32. New York: Plenum; 1986. 43-50.

Reed, R. P.; Read, D. T.; Tobler, R. L. Notch tensile measurements and fracture toughness correlations for austenitic stainless steel. Reed, R. P.; Clark, A. F., eds. Advances in Cryogenic Engineering--Materials, vol. 32. New York: Plenum; 1986; 361-368.

Reed, R. P.; Schramm, R. E. Fitness-for-service assessment of pipeline girth welds, with emphasis on nondestructive inspection. Goel, V. S., ed. The Mechanism of Fracture. Metals Park, Ohio: American Society for Metals; 1986. 255-263.

Reed, R. P.; Simon, N. J.; Purtscher, P. T.; Tobler, R. L. Alloy 316LN for low temperature structures: A summary of tensile and fracture data. Proceedings, Eleventh International Cryogenic Engineering conference. London: Butterworth Scientific. In press.

Reed, R. P.; Tobler, R. L. Proposed standard method for tensile testing of structural alloys at liquid helium temperature. Reed, R. P., ed. Materials Studies for Magnetic Fusion Energy Applications at Low Temperatures--IX. Nat. Bur. Stand. (U.S.) NBSIR 86-3050; 1986 May. 177-193.

Reed, R. P.; Walsh, R. P. Low temperature deformation of copper and an austenitic stainless steel. Reed, R. P.; Clark, A. F., eds. Advances in Cryogenic Engineering--Materials, vol. 32. New York: Plenum; 1986. 302-312.

Schramm, R. E.; Siewert, T. A. Production and sizing of uniform two-dimensional flaws in welds for NDE calibration. Mater. Eval. 44: 1136-1138; 1986.

Schramm, R. E.; Siewert, T. A. Sizing planar flaws in weldments using low-frequency EMATs. Thompson, D. O.; Chimenti, D. E., eds. Review of Progress in Quantitative Nondestructive Evaluation, vol. 5B. New York: Plenum; 1986. 1705-1712.

Shives, T. R.; Smith, L. C. Microindentation hardness measurements on metal powder particles. Blau, P. J.; Lawn, B. R., eds. Microhardness Indentation Technology in Materials Science and Engineering. Philadelphia, American Society for Testing and Materials, STP 889; 1986. 243-256.

Siewert, T. A. Predicting the toughness of SMA austenitic stainless steel welds at 77 K. Weld. J. 65: 23-29 (1986).

Simon, N. J.; Reed, R. P. Strength and toughness of AISI 304 and 316 at 4 K. J. Nucl. Mater. In press.

Tobler, R. L. Near-threshold fatigue crack growth behavior of AISI 316 stainless steel. Reed, R. P.; Clark, A. F., eds. Advances in Cryogenic Engineering--Materials, vol. 32. New York: Plenum; 1986. 321-327.

Tobler, R. L.; Cheng, Y.-W. Fully automatic near-threshold fatigue-crack growth rate measurements at liquid helium temperatures. Int. J. Frac. 7: 191-197; 1985.

Tobler, R. L.; Reed, R. P. Proposed standard method for fracture toughness testing of structural alloys at liquid helium temperatures. Reed, R. P., ed. Materials Studies for Magnetic Fusion Energy Applications at Low Temperatures--IX. Nat. Bur. Stand. (U.S.) NBSIR 86-3050; 1986 May. 195-207.

Tobler, R. L.; Shu, Q.-S. Fatigue crack initiation from notches in austenitic stainless steels. Cryogenics 26: 396-401; 1986.

Tobler, R. L.; Siewert, T. A.; McHenry, H. I. Strength-toughness relationship for austenitic stainless steel welds at 4 K. Cryogenics 26: 392-395.

Thomson, R.; Chuang, T.-J.; Lin, I.-H. The role of surface stress in fracture. Acta Metall. 34(6): 1133-1143; 1986.

SELECTED TECHNICAL AND PROFESSIONAL COMMITTEE LEADERSHIP

Advanced Materials Institute
- 1987 National Conference Committee
  - R. P. Reed

American Society for Metals
- Joining Division
  - T. A. Siewert, Government Liaison

American Society for Testing and Materials
- E24: Fracture Testing Committee
  - Proceedings, 18th National Symposium on Fracture Mechanics
    - D. T. Read, R. P. Reed, editors
  - E24.05: Terminology
    - R. deWit, Secretary
  - E24.06: Fracture Mechanics Applications
    - E24.06.04: Weld Testing
      - H. I. McHenry, Chairman
- E28: Mechanical Testing
  - E28.04: Tension Testing
    - E28.04.03: Verification of Alignment
      - B. W. Christ, Chairman
  - E28.06: Hardness
    - E28.06.04: Hardness Test Block Intercomparison Task Group
      - T. R. Shives, Chairman; R. J. Fields, Cochairman

American Welding Society
- Technical Papers Committee
  - T. A. Siewert
- Welding Journal
  - T. A. Siewert, Reviewer

American Welding Institute
- On-line Welding Data Base Committee
  - T. A. Siewert

Colorado School of Mines
- Steel Research Institute Advisory Board
  - R. P. Reed

International Cryogenic Materials Conference
- Board of Directors
  - R. P. Reed, Finance Officer
- Proceedings
  - R. P. Reed, Coeditor
- 1987 Conference Program Committee
  - M. B. Kasen

Mechanical Failures Prevention Group
- T. R. Shives, Executive Secretary
- S. R. Low, Committee member
- T. R. Shives, Proceedings Editor

Metals Properties Council
- Technical Advisory Committee
  - R. P. Reed, B. W. Christ
- Materials for Utilization at Cryogenic Temperatures Task Group
  - M. B. Kasen

Metallurgical Transactions
- Board of Review
  - H. M. Ledbetter

NBS-Boulder Editorial Review Board
- J. C. Moulder

U.S. Department of Energy, Office of Fusion Energy
- Analysis and Evaluation Task Group
  - N. J. Simon
- Joint U.S.-Japanese Exchange Program Advisory Committee
  - H. I. McHenry, R. P. Reed
- Low-Temperature Materials for Magnetic Fusion Energy Committee
  - R. P. Reed, Coordinator

Versailles Project on Advanced Materials and Standards Task Group
- Cryogenic Structural Materials Working Group
  - R. P. Reed
- Technical Working Area, Weld Characteristics
  - H. I. McHenry, Chairman
  - M. B. Kasen

Welding Research Council
- Data Base Task Group
  - T. A. Siewert
- Materials and Welding Procedures Subcommittee
  - T. A. Siewert

INDUSTRIAL AND ACADEMIC INTERACTIONS

Industrial Interactions

In response to numerous requests from designers in industry, members of our division have supplied data and references on properties of specific materials and advice on material selection, data interpretation, measurement techniques, and welding procedures. Our expertise has been utilized in wind tunnel design, space instrumentation, accelerator design, cryogenic tankage, aerospace, and advanced aircraft applications. We are a major source of materials data at cryogenic temperatures. We provided handbook data on the cryogenic properties of stainless steel alloys to many industries. Our excellent test facilities are often used by industrial personnel. These small requests accrue to a significant assistance to industry.

1. American Iron and Steel Institute

   The American Iron and Steel Institute (AISI) Cooperative Technology Unit on Modeling and Performance of Rolling Mills is acting as a steel industry liaison group to interact with NBS researchers on thermomechanical processing. The AISI group is polling the steel industry to establish specific research priorities. They will define the processing conditions representative of current mill practice, identify the industry's most urgent needs, and estimate the value of the research results.

2. American Welding Institute

   The division has provided assistance to the American Welding Institute (AWI) during its formative period. This organization was established to improve the transfer of the latest welding technology into United States industry. This year NBS and AWI hosted a workshop on Computerization of Welding Data to determine the best organization of data for the goal of increasing the productivity of our nation. Over forty participants, representing diverse interests within the welding industry, produced a ranked list of the welding data needs and defined the users of this information. The publication of the workshop results will help to unify the United States effort in the computerization of welding data.

3. Fermi National Accelerator Laboratory

   The division supplied critically evaluated cryogenic material property data for Fermi National Accelerator Laboratory for use in their design of the dipole magnet cryostat system for the proposed Superconducting Super Collider (SSC). The SSC is a 40-TeV proton-antiproton accelerator that will employ a string of about 10,000 superconducting magnets around a circumference of approximately 100 km (62 mi.). Tensile, elastic, and fracture properties were supplied for eleven structural alloys and two composites from 300 to 4 K. A comparative analysis of thermal property data from 300 to 4 K was supplied for titanium, aluminum, stainless steel, and copper alloy groups.

4. Ford Motor Company

Under the auspices of the U.S. Department of Commerce Science and Technology Fellowship Program, B. W. Christ of our division was appointed a "Com-Sci Fellow" in the Ford Scientific and Engineering Laboratories from July 1, 1985 until June 30, 1986. He participated in a cooperative study that reviewed structural designs and manufacturing processes prescribed by existing codes and standards and determined how technology transfer can lead to manufacturing cost reductions through modifications of design, materials selection, and manufacturing processes. These potential savings have been previously identified in the 1983 NBS report "The Economic Effects of Fracture in the United States." B. W. Christ visited and toured Ford and other automotive companies to learn firsthand how a manufacturing industry addresses the problems of structural materials durability, such as, wear, corrosion, and fatigue and fracture. At the same time, he consulted with industry engineers and explained how existing input-output economics data about nationwide costs of corrosion and fracture can be useful in planning technology transfers, and further, made suggestions about plausible technology transfers beneficial to the domestic motor vehicle industry.

5. Naval Research Laboratory

A. V. Clark collaborated with researchers at the Naval Research Laboratory, Washington, D.C. on the use of Rayleigh waves for measurements of surface residual stress and texture. A theory was developed that accounted for slight anisotropy as well as stress on Rayleigh wave velocity. Variation of velocity with propagation directions was then measured on unstressed plates to characterize texture. Results were in good agreement with bulk measurements.

6. Rockwell International

We have a major low-temperature test program to measure the mechanical properties of selected titanium alloys, which are the main structural material for aerospace containers of liquefied hydrogen. The program will examine the effects of different thermomechanical processes on the mechanical properties of these alloys at 20 K. Research has concentrated on tensile and notch tensile measurements of Ti-5Al-2.5Sn at 20 K; low-temperature elastic constants of Ti-Al-Sn alloys have been measured. Low- and high-cycle fatigue equipment for testing at 20 K has been assembled for the next phase of this program.

7. Welding Research Council

The Welding Research Council (WRC) and NBS have established a joint program to produce nationally recognized weld procedures. The WRC is producing a series of welds that are representative of production welds. These welds, sectioned according to fabrication code requirements, are

sent to NBS, which is serving as a nationally known, impartial testing laboratory capable of meeting the various accuracy and identification requirements. Our support for this program has increased from the testing of 200 specimens in 1985 to testing more than 500 specimens in 1986. The WRC is currently reviewing the data from these tests and preparing the first weld procedure specifications. Eventually, these specifications will eliminate the costly and time-consuming individual tests for structural integrity now required of welding contractors.

Joint Industrial and Academic Interactions

1. Steel Research Center

The Steel Research Center is a center for cooperative research of industries and universities that was established at the Colorado School of Mines in 1984 to establish research programs, educational programs, and technology transfer for the benefit of the steel industry. As a charter member, NBS obtained access to a forum of steel producers and users that helps to guide our research on thermomechanical processing of steels and development of cryogenic alloys. At the request of the American Iron and Steel Institute, we are exploring the development of cooperative programs between NBS and the Steel Research Center in the area of thermomechanical processing of steel.

2. Aluminum Company of America and Iowa State University

A. V. Clark is collaborating with scientists at the ALCOA Research Center and Ames Laboratory, Iowa State University. The purpose of the collaboration is to develop and ultrasonic instrument for on-line texture monitoring of material used in aluminum can manufacture.

Academic Interactions

1. Colorado State University

J. C. Moulder and D. T. Read collaborated with J. F. Cardenas-Garcia of Colorado State University in calculating J-integrals from full-field strain measurements. They analyzed experimental data for an HSLA steel panel and a 5052 aluminum alloy and verified the path independence of the J-integral in both cases.

2. Pennsylvania State University

T. A. Siewert is working with S. Liu of Pennsylvania State University in the study of droplet transfer frequency in welding arcs. This study is revealing the physical basis for qualitative descriptions of the voltage and current values that produce acceptable welds. Arc extinction and reignition patterns determine the arc stability and so the weld spatter, one measure of an acceptable weld.

3. Stanford University

J. C. Moulder collaborates with B. A. Auld of Stanford University on comparisons of theory and experiment in eddy-current nondestructive evaluation. This year they modeled eddy-current reflection probes and developed calibration methods and standards.

4. University of Colorado

A. V. Clark and R. E. Schramm worked with S. K. Datta of the Department of Mechanical Engineering and CIRES at the University of Colorado in Boulder to calculate reflection and transmission coefficients for ultrasonic signals scattered by canted flaws in steel plates. These analyses and their comparison with experiment help to determine the optimum geometry of EMAT placement for flaw sizing.

H. M. Ledbetter collaborates with S. K. Datta of the University of Colorado on theoretical studies of composite-material physical properties: sound velocities, elastic constants, and internal friction. Currently they are studying composite-material interfaces, especially with regard to sound velocities and damping at finite frequencies.

5. University of South Carolina

H. M. Ledbetter collaborated with T. Datta on theoretical and experimental studies of low-temperature austenitic-steel physical properties, especially elastic constants and magnetic susceptibility. In these materials, physical properties (and perhaps plastic-deformation properties) depend on the magnetic state, which may be paramagnetic, antiferromagnetic, spin glass, or other.

H. M. Ledbetter collaborates with R. Edge on studies of the low-temperature magnetic state in Fe-Cr-Ni alloys. Recently, at Oak Ridge National Laboratory, they obtained exciting new neutron-diffraction results, which they are now trying to interpret.

APPENDIX

U.S. DEPARTMENT OF COMMERCE
National Bureau of Standards

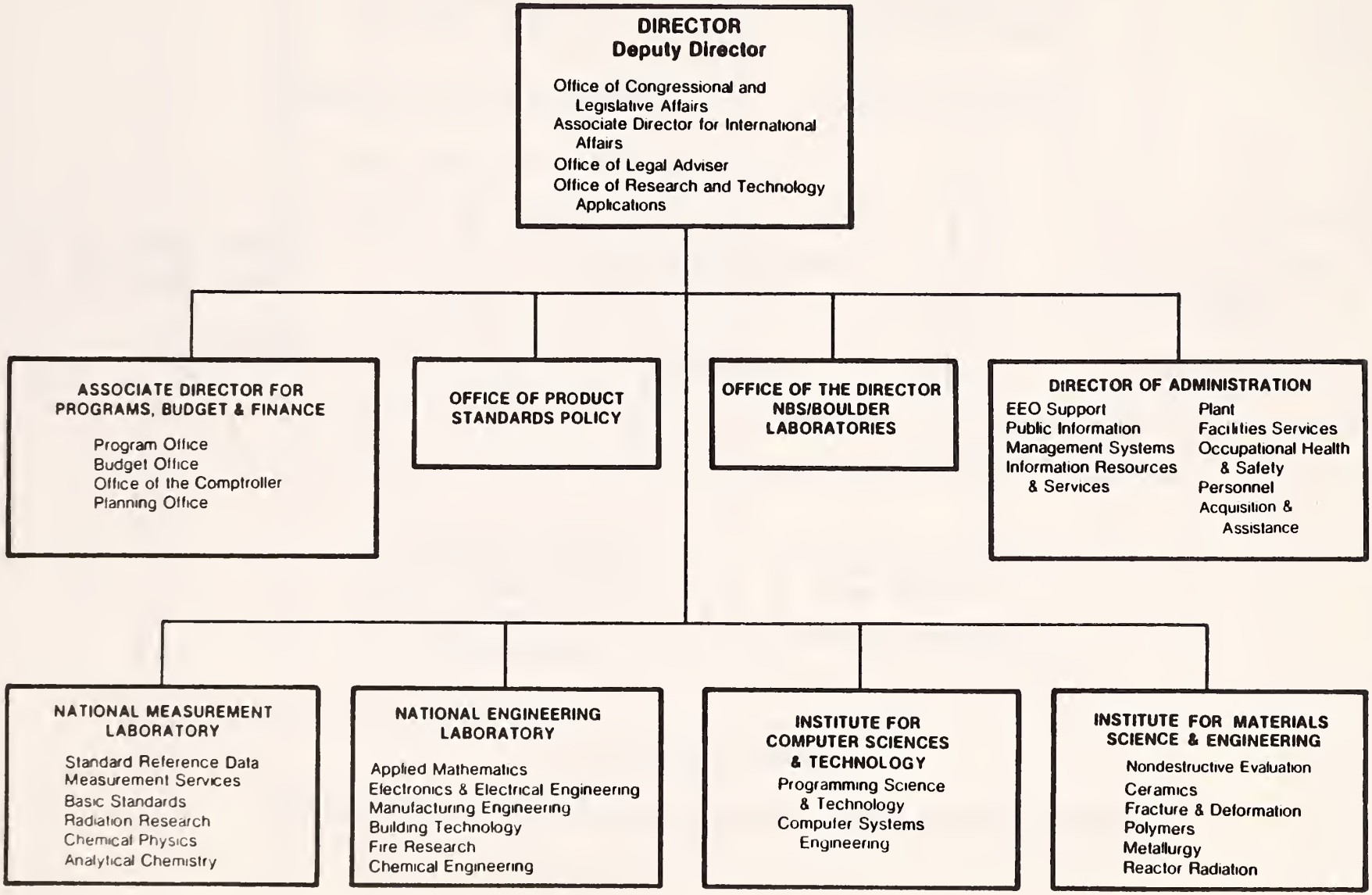

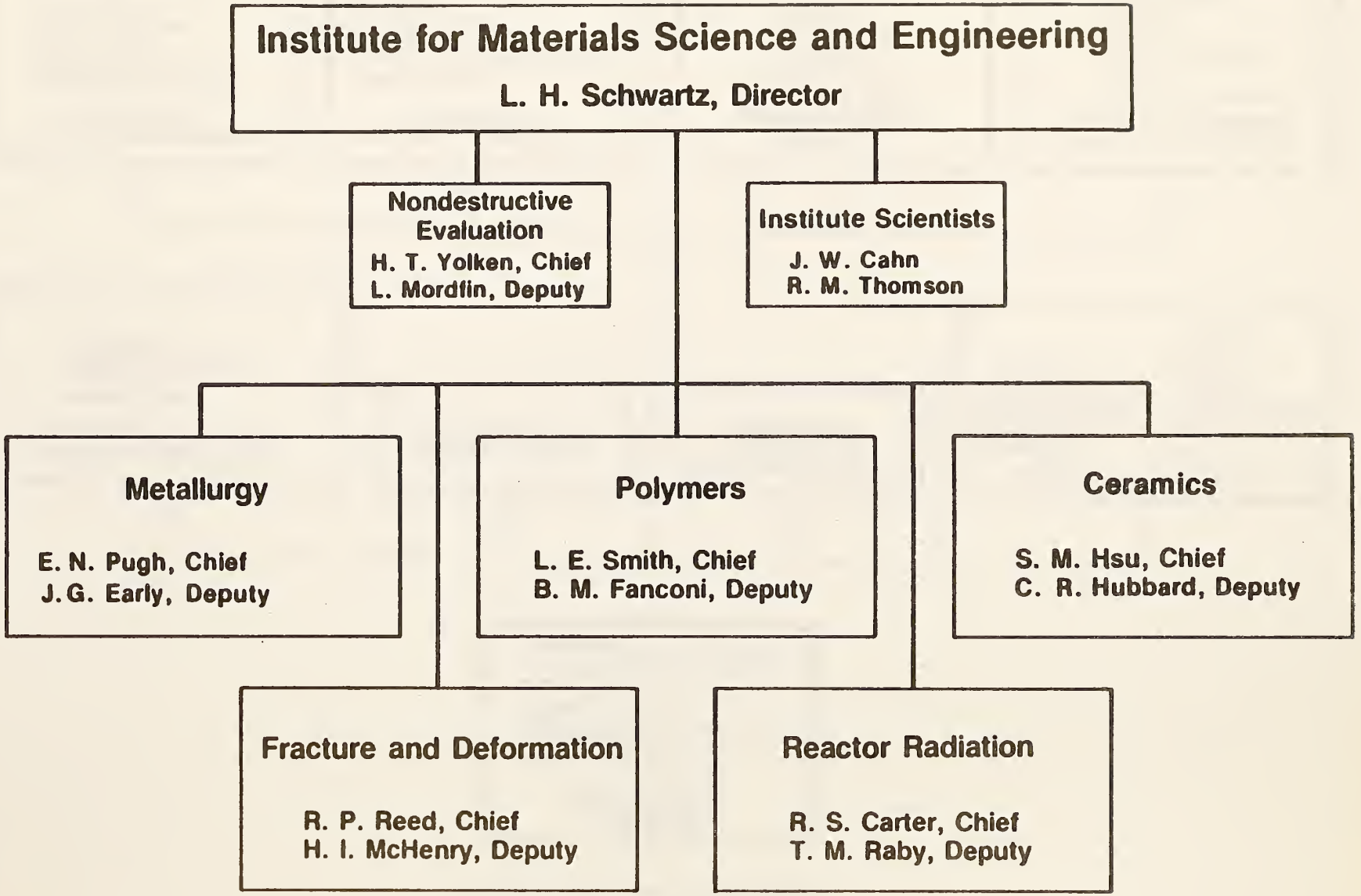
Institute for Materials Science and Engineering
L. H. Schwartz, Director
Nondestructive Evaluation
H. T. Yolken, Chief
L. Mordfin, Deputy
Institute Scientists
J. W. Cahn
R. M. Thomson
Metallurgy
E. N. Pugh, Chief
J. G. Early, Deputy
Polymers
L. E. Smith, Chief
B. M. Fanconi, Deputy
Ceramics
S. M. Hsu, Chief
C. R. Hubbard, Deputy
Fracture and Deformation
R. P. Reed, Chief
H. I. McHenry, Deputy
Reactor Radiation
R. S. Carter, Chief
T. M. Raby, Deputy

NBS-114A (REV. 2-8C)

U.S. DEPT. OF COMM. BIBLIOGRAPHIC DATA SHEET (See instructions)	1. PUBLICATION OR REPORT NO. NBSIR 86-3436	2. Performing Organ. Report No.	3. Publication Date OCTOBER 1986

4. TITLE AND SUBTITLE

Institute for Materials Science and Engineering
Fracture and Deformation Division
Technical Activities 1986

5. AUTHOR(S)

6. PERFORMING ORGANIZATION (If joint or other than NBS, see instructions)

NATIONAL BUREAU OF STANDARDS
DEPARTMENT OF COMMERCE
WASHINGTON, D.C. 20234

7. Contract/Grant No.

8. Type of Report & Period Covered

9. SPONSORING ORGANIZATION NAME AND COMPLETE ADDRESS (Street, City, State, ZIP)

NBS - Fracture and Deformation Division, 430
Room 1601/Building 2
325 Broadway
Boulder, CO 80303

10. SUPPLEMENTARY NOTES

[ ] Document describes a computer program; SF-185, FIPS Software Summary, is attached.

11. ABSTRACT (A 200-word or less factual summary of most significant information. If document includes a significant bibliography or literature survey, mention it here)

This report summarizes the technical program of the Fracture and Deformation Division of the Institute for Materials Science and Engineering, National Bureau of Standards for the fiscal year 1986. The division's two major program areas are elastic-plastic fracture mechanics and fracture mechanisms and analysis. Elastic-plastic fracture mechanics includes contributions from stress analysis, material properties, nondestructive evaluation, and welding. Division efforts in fracture physics, time-dependent properties, composite mechanics, mechanical metallurgy, physical properties, and material performance compose the second area, fracture mechanisms and analysis. Significant technical programs relating to each of these are presented. Major accomplishments are highlighted, including an interdisciplinary analysis of a major pressure vessel failure, extensive collaboration with the automotive industry to reduce costs associated with failure, successful large-scale experiments of dynamic crack arrest, and composite-modeling, material-property, and test-development research.

The report includes the division's professional staff and their research areas, publications, leadership in professional societies, and collaboration in research programs with industries and universities.

12. KEY WORDS (Six to twelve entries; alphabetical order; capitalize only proper names; and separate key words by semicolons)

Annual report; composites; deformation; fracture mechanics; fracture physics; welding

13. AVAILABILITY

[X] Unlimited

[ ] For Official Distribution. Do Not Release to NTIS

[ ] Order From Superintendent of Documents, U.S. Government Printing Office, Washington, D.C. 20402.

[X] Order From National Technical Information Service (NTIS), Springfield, VA. 22161

14. NO. OF PRINTED PAGES 73

15. Price $11.95

USCOMM-DC 6043-P80